Molecular Basis of the Ligand-binding Specificity of αvβ8 integrin

（αvβ8 インテグリンのリガンド結合特異性の分子基盤）

A Thesis for Doctor Degree

Presented to Osaka University

2018

Akio Ozawa

Table of Contents

Abbreviations

BSA, bovine serum albumin

BI, β I-like domain

CBB, Coomassie Brilliant Blue

DLL, disulfide-linked loop

DMEM, Dulbecco's modified Eagle's medium

ECM, extracellular matrix

EGF, epidermal growth factor

ELISA, enzyme-linked immuno-sorbent assay

ER, endoplasmic reticulum

GF, growth factor

HYB, β hybrid domain

LAP, latency-associated peptide

mAb, monoclonal antibody

MIDAS, metal ion dependent adhesion site

MMP, matrix metalloproteinase

Ni-NTA, nickel-nitrilotriacetic acid

pAb, polyclonal antibody

PBS, phosphate-buffered saline

PPC, proprotein convertase

RGD, arginine-glycine-aspartic acid

SDS-PAGE, sodium dodecyl sulfate-polyacrylamide gel electrophoresis

TB, TGF-β-binding

TBS, Tris-buffered saline

TGF, transforming growth factor

Summary

αvβ8 is an integrin that recognizes an Arg-Gly-Asp (RGD) motif and interacts with fibronectin, vitronectin, and latent TGF-β1. I comprehensively determined the binding activity of αvβ8 integrin towards 25 putative secreted proteins having an RGD motif conserved among vertebrates. αvβ8 integrin strongly and preferentially bound to latent TGF-β1 with an apparent dissociation constant of 2.3 ± 0.2 nM, but showed only marginal activity to other RGD-containing proteins including fibronectin and vitronectin. Site-directed mutagenesis of latent TGF-β1 demonstrated that the high-affinity binding of αvβ8 integrin to latent TGF-β1 was defined by Leu-218 immediately following the RGD motif within the latency-associated peptide of TGF-β1. A 9-mer synthetic peptide containing an RGDL sequence strongly inhibited interactions of latent TGF-β1 with αvβ8 integrin, while a 9-mer peptide with an RGDA sequence was ~60-fold less inhibitory. Consistent with the critical role of Leu-218 in latent TGF-β1 recognition by αvβ8 integrin, the high-affinity binding toward αvβ8 integrin was conferred on fibronectin by substitution of its RGDS motif with an RGDL sequence. Because αvβ3 integrin neither exhibited strong binding to latent TGF-β1 nor distinguished the difference between the RGDL- and RGDA-containing peptides, it is less likely that the common subunit, αv, is involved in the recognition of Leu-218. Therefore, I explored whether Leu-218 is recognized by the integrin β8 subunit. To this end, I produced a series of swap mutants of integrin β8 and β3 subunits and examined the interaction of these mutants with latent TGF-β1. The results indicated that the β8 I-like domain primarily defines the high affinity binding of latent TGF-β1 to αvβ8 integrin. Taken together, our results provide evidence that the high-affinity binding of αvβ8 integrin with latent TGF-β1 was ensured by the interaction between Leu-218 residue and β8 I-like domain, with the former serving as an auxiliary recognition residue defining the restricted ligand specificity of αvβ8 integrin toward latent TGF-β1.

Introduction

I. The Extracellular Matrix

In multicellular organisms, tissues contain not only cells but also extracellular matrices (ECMs) that fill up most extracellular space. Cells produce and assemble ECM components into an organized meshwork in their proximity. The ECM had been defined morphologically as extracellular material visible as fibrils or sheets by the electron microscopic observation. Nowadays it can be defined more broadly to include almost all secreted molecules that are immobilized outside cells, *e.g.* TGF-β1 (Reichardt, 1999). There are two types of ECM: one is basement membrane that underlies almost all epithelial and endothelial cells and surrounds muscle and neuronal cells; the other is interstitial matrix that surrounds all cells existing in connective tissues. The basement membrane is a sheet-like structure constituted of ECM proteins and separates the epithelium from underlying connective tissues. Thus, the basement membrane is the ECM directly associated with epithelial cells that play essential roles in individual organs, while the interstitial matrices provide mechanical support and physical strength to connective tissue as a whole.

The ECM had been thought to function merely as materials filling the space between cells. However, recent studies revealed that the ECMs play pivotal roles in cell survival, proliferation, and migration, and are involved in diverse biological processes including organogenesis, thus regarded as an essential factor that regulates behaviors of cells (Reichardt, 1999). The functions of ECMs are now summarized as follows; 1) providing the mechanical integrity, rigidity, and elasticity for tissues to endure the force or impact from the surroundings; 2) providing adhesive substrates for cells to transmit adhesion signals that are essential for cells to survive; and 3) sequestering soluble factors, such as growth factors and morphogens, to help

regulate the spatial and temporal properties of signals conveyed by these factors.

II. The Integrins : a Family of Receptor Proteins for ECMs

Integrins are a family of adhesion receptors that bind to a variety of extracellular ligands, typically cell-adhesion proteins in the ECM (Pytela et al., 1985b). Integrins are composed of two non-covalently associated subunits, termed α and β. By integrating the information of extracellular proteins and the intracellular signaling cascades, integrins play mandatory roles in embryonic development and the maintenance of tissue architecture by providing essential links between cells and the ECM (Hynes, 2002).

II-1. Integrin Structure

One α and one β subunits noncovalently associate with each other to form α-β heterodimeric receptors (Xiong et al., 2001). Amino acid sequences and electron microscopic observations of purified integrin heterodimers revealed that integrins consist of a large extracellular domain with a globular head region and two long tails each containing a transmembrane domain and an unstructured cytoplasmic tail domain (**Figure 1A**) (Nermut et al., 1988). The β-propeller domain of the α subunit consists of seven segments. Each of the segments forms a blade-like β-sheet structure (blade I~VII) consisting of four β-strands (Xiong et al., 2001). Nine α subunits (α1/2/10/11/D/E/L/M/X) contain an additional domain called α I-domain between blade II and III of the β-propeller domain. The I-like domain of β subunit (β I-like domain), a similar structure to the α I-domain, contains a ligand-binding site. The head region composed of the β-propeller domain of α subunit and the β I-like domain forms a ligand-binding site while the C-terminal tail functions as a scaffold for signal-transducing molecules such as actin-binding proteins, adapter proteins, and kinase proteins (Arnaout et al., 2007; Hynes, 2002). The range of motion of the leg region is broad, providing the “integrin flexibility” and enabling them to modulate the ligand-binding affinity of integrins.

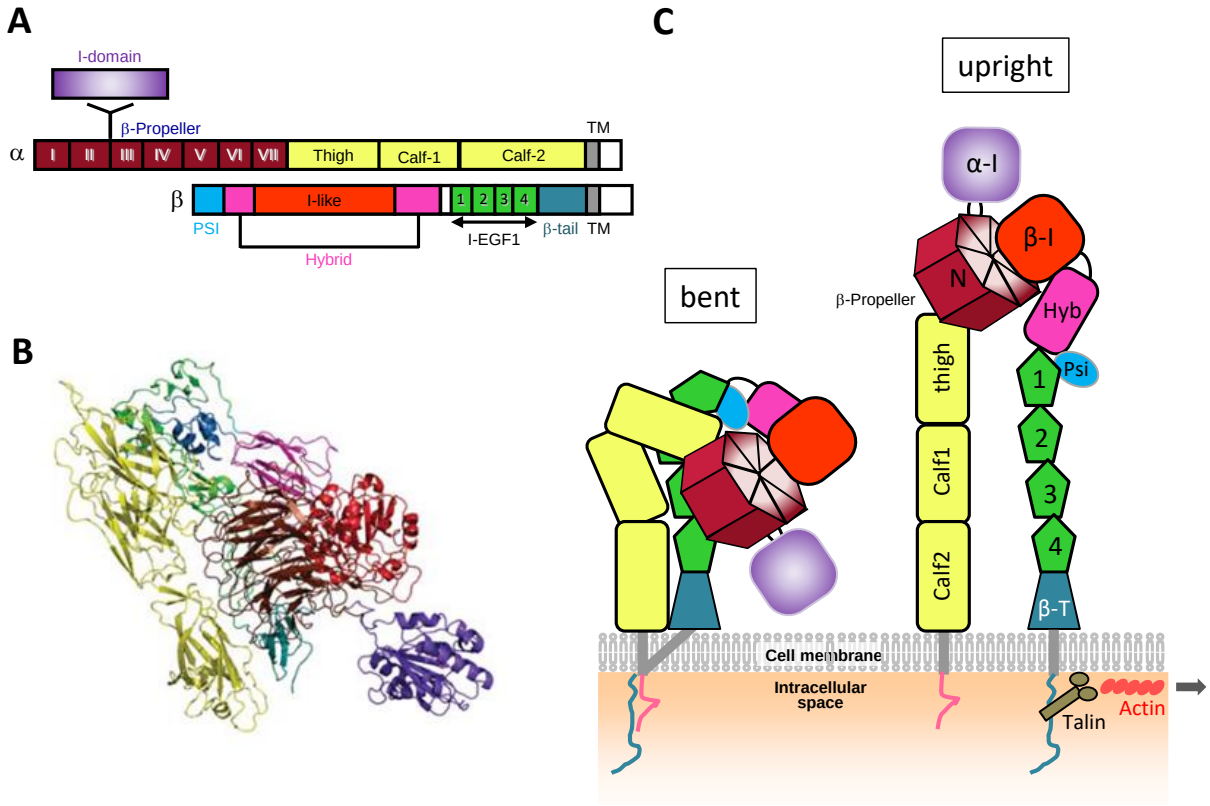

Figure 1. Integrin structure. (*A*) Domain structure of typical integrin α and β subunits (Xie *et al*., 2009). PSI, plexin-semaphorin-integrin; I-EGF, integrin-EGF; TM, transmembrane domain. (*B*) Structure of αxβ2 using the same color code in A (drawn with PyMOL [DeLano Scientific] using PDB coordinates 3K6S). (*C*) Conformational change of the αxβ2 integrin on activation. The integrin adopts a bent and upright conformation in low-affinity and high-affinity state, respectively. These figures were modified from Campbell and Humphries (2011), "Integrin Structure, Activation, and Interaction," in Hynes and Yamada, eds., *Exrtracellular Matrix Biology*, Cold Spring Harbor Laboratory Press, p. 170.

Integrins exist in an equilibrium between a bent low-affinity state and an upright high-affinity state. The crystal structures of αvβ3, αIIbβ3 and αxβ2 have been determined and are all in a similar conformation that would place the αβ headpiece near the membrane surface (**Figure 1B and C**). Integrin can be activated by the binding of ECM ligands to its ectodomains (known as 'outside-in' activation) or by the binding of the talin head domain to β-integrin cytoplasmic tail and acidic membrane phospholipids (known as 'inside-out' activation). These activations lead to conformation rearrangement in the ectodomain through pulling the integrin β subunit cytoplasmic tail by actin filaments, resulting in extension of the α and β subunits (**Figure 1C**). This model for the conformational changes of integrin on activation is proposed by an electron-microscopic study of αIIbβ3 integrin embedded in

membrane nanodiscs (Beglova et al., 2002). There is strong evidence indicating that the conformational change occurring in the β-I/hybrid region of β3 subunit is required for high-affinity binding of αIIbβ3 integrin to its ligands. The interaction of αIIbβ3 integrin with its ligands initiates the conformational rearrangement, *i.e.*, structural alteration in β3 I-like domain. The downward movement of the β3-I α7-helix toward the hybrid domain, in turn, initiates a swing-out motion of the β hybrid domain away from αIIb subunit (Cheng et al., 2013) (**Figure 2**). As a result, the αIIbβ3 integrin shifts from low-affinity to high-affinity state.

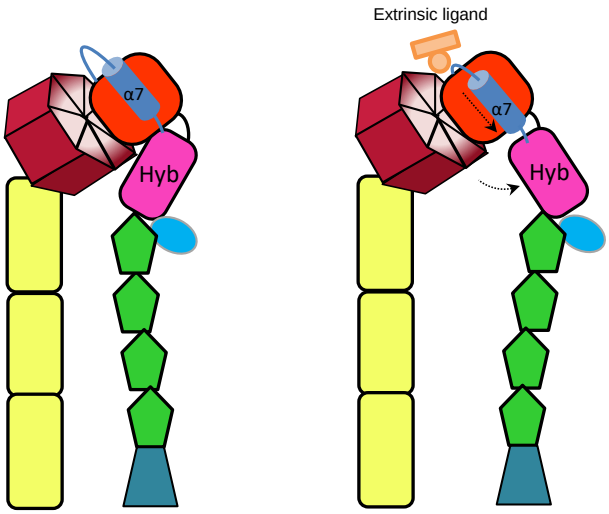

Figure 2. An illustration of the movement of the α7 helix in the I-like domain of β subunit and the swing-out of the hybrid domain (the domains are defined in Figure 1). This model corresponds to the closed (*left*) and open (*right*) conformations of an αIIbβ3 integrin. Figure was modified from Cheng *et al*., 2013.

II-2. The Diversity of Integrin Subunits and Their Interactions

In mammals, 18 α and 8 β subunits have been identified and combinations of these subunits give rise to at least 24 distinct integrin heterodimers, among which 18 isoforms function as ECM receptors. Ligand-binding specificities of integrins are determined by the combination of the α and β subunits (Takada et al., 2007) (**Figure 3**). Based on their ligand-binding specificities, integrins can be classified into five groups: laminin-binding type (α3β1, α6β1, α6β4, and α7β1), Arg-Gly-Asp (RGD)-binding type (α5β1, αVβ1/3/5/6/8, α8β1, and αIIbβ3), collagen-binding type (α1β1, α2β1, α10β1, and α11β1) (Pytela et al., 1985b), Leu-Asp-Val (LDV) or Ile-Asp-Gly (IDG)-binding type (α4β1, α4β7, and α9β1), and

leukocyte-specific type (the four members of the β2 superfamily, and αEβ7). α4- and α9-containing integrins have been shown to interact with the sequences comprised of aliphatic residues adjacent to acidic residues, such as LDV or IDG (Komoriya et al., 1991; Schneider et al., 1998; Yokosaki et al., 1998). This classification also reflects ligand-binding specificities of individual integrins, thus showing their specific, non-redundant functions. This is also shown physiologically using integrin gene knockout mice (**Table 1**). To date, genes for all integrin α and β subunits have been knocked out, and each phenotype is distinct, reflecting the different roles among the various integrins.

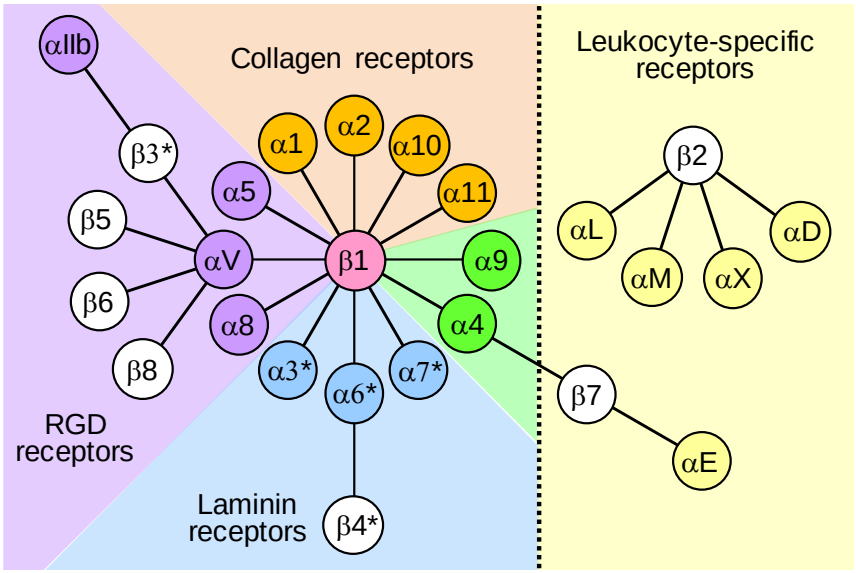

Figure 3. The combinations of integrin α and β subunits and their binding specificities. The mammalian subunits and their αβ associations; 8 β subunits can assort with 18 α subunits to form 24 distinct integrin isoforms. They are fallen into 5 general categories; laminin-binding type (*light blue*), RGD-binding type (*purple*), collagen-binding type (*orange*), LDV/IDG-binding type (*green*), and leukocyte-specific type (*yellow*). There are 5 isoforms specifically expressed in leucocytes. Some subunits show alternatively spliced isoforms (*). All but leukocyte-specific integrins are receptors for ECM proteins. Most integrins are capable of binding multiple ligands, and there are many others beyond those shown here (Humphries *et al*. 2006). αv integrins are known as an activator and regulator for TGF-β. Figure was modified from Hynes, 2002.

Table 1. Integrin gene knockout phenotypes

Subunit	Lethality	Phenotypes
α1	viable, fertile	No immediately obvious developmental defects, reduced tumor vascularization
α2	viable, fertile	Few immediately obvious developmental defects, displayed platelet aggregation and reduced binding to monomeric collagen, reduced mammary gland branching
α3	perinatal lethal	Kidney tubule defects, reduced branching morphogenesis in lungs, mild skin blistering, lamination defects in neocortex
α4	E11/14 lethal	Defects in placenta (chorioallantoic fusion defect) and heart (epicardium, coronary vessels)
α5	E10-11 lethal	Defects in mesoderm (posterior somites) and vascular development, neural crest apoptosis
α6	perinatal lethal	Severe skin blistering, other epithelial tissues also defective. Lamination defects in cortex and retina
α7	viable, fertile	Muscular dystrophy, defective myotendinous junctions
α8	perinatal lethal	Smaller or absent kidneys, inner hair cell defects
α9	viable	Die within 10 days of birth, chylothorax due to lymphatic duct defect
α10	viable, fertile	Growth retardation of the long bones due to moderate dysfunction of growth plate chondrocytes
α11	viable, fertile	Dwarfism with increased mortality due to severely defective incisors
αv	E10/perinatal lethal	Two classes; embryonic lethality due to placental defects, perinatal lethality with cerebral vascular defects probably due to neuroepithelial defects, cleft palate
αIIb	viable, fertile	Hemorrhage, no platelet aggregation
αL	viable, fertile	Impaired leukocyte recruitment
αM	viable, fertile	Defective phagocytosis and apoptosis of neutrophils, mast cell development defects, adipose accumulation
αX	viable, fertile	Decreased longevity and survival rate upon infection with pneumococci
αD	viable, fertile	No immediately obvious developmental defects, reduced T cell response and phenotypic changes after induction by Staphylococcal enterotoxin
αE	viable, fertile	Greatly reduced numbers of intraepithelial lymphocytes
β1	E6.5 lethal	Peri-implantation lethality, inner cell mass deteriorates, embryo fail to gastrulate
β2	viable, fertile	Leukocytosis, impaired inflammatory responses, skin infections, T cell proliferation defects
β3	viable, fertile	Hemorrhage, no platelet aggregation, osteosclerosis, hypervascularisation of tumors
β4	perinatal lethal	Severe skin blistering, other epithelial tissues also defective.
β5	viable, fertile	No immediately obvious developmental defects
β6	viable, fertile	Inflammation in skin and airways, impaired ling fibrosis, all probably due to failure to active TGF-β
β7	viable	deficits in gut-associated lymphocytes-no Peyer's patches, reduced intraepithelial lymphocytes
β8	E10/perinatal lethal	Two classes; embryonic lethality due to placental defects, perinatal lethality with cerebral vascular defects probably due to neuroepithelial defects

This table is cited from Ivaska *et al*., 2013.

II-3. Fine-tuning of Ligand-binding Specificity by Integrin β-subunit

Although it has been shown that the ligand-binding specificity of individual integrin isoforms is principally dependent on their α subunits (Barczyk et al., 2010b) (**Figure 3**), accumulating data suggest that the integrin β subunits also fine-tune the ligand binding preference of integrins by enhancing or attenuating their binding affinities toward specific ligands (Humphries et al., 2006). The ligand RGD peptide binds at the junction between the α and β subunits, where the Asp residue of the peptide coordinates the divalent cation in β I-like domain, making it likely that the β I-like domain is directly involved in ligand recognition by αvβ3 and αIIbβ3 integrins (see below **Chapter III-1**) (Cheng et al., 2013; Xiao et al., 2004; Xiong et al., 2002). For example, although α6β4 integrin shares the same α subunit with α6β1, it displays a distinct binding specificity toward a panel of laminin isoforms containing distinct α chains (Nishiuchi et al., 2006). The β I-like domains of β1, β2, β3, β5, β6 and β8 subunits contain a small disulfide-linked loop (designated DLL, **Figure 4**), which is predicted to be located close to the α-β interface and involved in determining ligand-binding specificity. Ligand-binding specificities of αvβ3 and αvβ1 integrins toward von Willebrand factor and fibrinogen were reversed via partial swapping of their DLL regions in the β I-like domain (Takagi et al., 1997a).

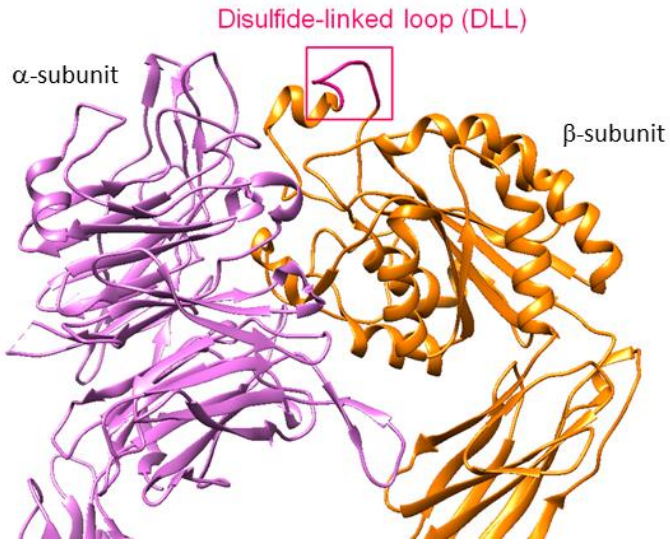

Figure 4. The structure of the head piece of αvβ6 integrin. αv and β6 subunits are labeled *purple* and *orange*, respectively. The disulfide-linked loop (DLL) is boxed and shown in *magenta*. DLL is located close to the junction between α and β subunits. The structure was displayed by Chimera (PDB ID; 4UM9).

II-4. Recognition Sequences of Integrins

The RGD cell-adhesive motif, a well known integrin ligand, was initially identified in fibronectin (Pierschbacher & Ruoslathi., 1984). Subsequently, several other ligands or sequences critical for integrin recognition have been identified, as shown in **Table 2**. α5β1, α8β1, αIIbβ3, and all five αv-containing integrins recognize the ligands containing an RGD motif. Crystal structures of αvβ3 and αIIbβ3 complexed with RGD peptides have been determined and provided the molecular basis for this binding (Xiao et al., 2004; Xiong et al., 2002). In addition to the RGD motif, αIIbβ3 integrin binds to the KQAGDV sequence present in the C-terminal region of γ chain of fibrinogen (Calvete et al., 1992; Springer et al., 2008). α4β1, α4β7, and α9β1 recognize an LDV motif, which is functionally similar to the RGD motif (Humphries et al., 2006). Fibronectin contains at least three distinct sequences that bind

Table 2. Integrin recognition sequences

Integrin	Representative adhesive ligand	Peptide sequence	Auxiliary sequence required for affinity modulation
α2β1	collagen	GFOG**E**R	
α4β1	emilin, fibronectin, VCAM-1	EXX**E**, L**D**V, I**D**S	
α9β1	polydom, emilin, tenascin, VCAM-1	EDDMM**E**VPY, EGL**E**, EI**D**G	
αvβ1	fibronectin, vitronectin	RG**D**	
αvβ3	fibronectin, vitronectin, fibrinogen, osteopontin, bone sialoprotein, fibrillin, EDIL-3, lactadherin, nephronectin, thrombospondin, tenascin-C, prothrombin, latent TGF-β1, vWF	RG**D**	
αvβ5	fibronectin, vitronectin, latent TGF-β1	RG**D**	
αvβ6	fibronectin, vitronectin, latent TGF-β1 fibrillin, tenascin-C	RG**D**	LXXL/I
α5β1	fibronectin	RG**D**	PHSRN and other basic residues
αIIbβ3	fibrinogen, fibronectin, vitronectin	RG**D**, KQAG**D**V	
α8β1	nephronecrin, fibronectin, vitronectin, osteopontin	RG**D**	LFEIFEIER
αMβ2	fibrinogen, C3bi	QKRL**D**GS	
α4β7	fibronectin, VCAM-1, MAdCAM	EIL**D**V	

The critical acidic residues are shown in *bold*.

to α4β1; LDV in the type III-connecting segment 1 (CS1), IDA in the heparin-binding domain 2, and EDGIHEL in the extra domain A (Komoriya et al., 1991; Schneider et al., 1998; Yokosaki et al., 1998). The key sites for binding to α4β1 in VCAM-1 are identified as IDS, which is homologous to LDV and IDA of fibronectin (Clements et al., 1994). Mutagenesis studies suggest that the binding of emilin-1 gC1q domain to α4β1 integrin mainly depends on a single Glu-933 residue that is highly conserved among a wide range of species (Verdone et al., 2008). Recently, Sato-Nishiuchi et al (2012) revealed that α9β1 integrin recognizes the EDDMMEVPY sequence, within which Glu-2641 is the critical acidic residue involved in the polydom recognition by α9β1 integrin. Structures of the α4- and α9- integrin subfamilies are uncharacterized, but it seems likely that the acidic residue within these binding motifs plays a critical role for coordinating a cation bound in the β I-like domain. α1, α2, α10, and α11 subunits containing an α I-domain dimerize with β1 subunit and form a distinct collagen-binding subfamily. A crystal structure of an α2 I-domain complexed with a triple-helical collagenous peptide has revealed that a Glu residue within the collagenous motif (*i.e.*, GFOGER) plays a critical role in forming a coordination bond with a metal cation (Emsley et al., 2000). α3β1, α6β1, α6β4, and α7β1 are classified as members of the laminin-binding integrins. Although the recognition sequence or peptide ligands have not been identified in the laminin-binding integrins, recent studies have demonstrated that the Glu residue at the third position from the carboxyl terminus of γ1 chain is critically required for the laminin-integrin interaction (Ido et al., 2007; Taniguchi et al., 2017; Takizawa et al., 2017).

III. RGD-binding Integrins

The RGD-binding integrins include α5β1, α8β1, αIIbβ3, and five αv-containing integrins, which interact with a variety of ECM ligands containing RGD motif(s) with distinct binding specificities. The αv-containing integrins are the most promiscuous among the family. Notably, αvβ3 integrin binds to a large number of extracellular matrix and other secreted proteins.

Although the αvβ3 integrin interacts with many RGD ligands, the molecular basis for such promiscuous binding specificity of the αvβ3 integrin remains to be elucidated.

III-1. Ligand Recognition Mechanisms by RGD-binding Integrins

Crystal structures of αvβ3 and αIIbβ3 integrins complexed with a cyclic RGD peptide have provided structural insights into the integrin-ligand interaction and greatly advanced our understanding of the mechanisms by which integrins recognize their ligands (Xiao et al., 2004; Xiong et al., 2002) (**Figure 5**). RGD peptide binds at an interface between the α and β subunits, in which the Arg residue fits into a cleft in a β-propeller domain in the α subunit and the Asp side chain coordinates the divalent cation at the metal ion-dependent adhesion site (designated as 'MIDAS') in β I-like domain (**Figure 5B**). Since all of the recognition sequences identified thus far have at least one acidic residue (aspartate or glutamate; see **Table 2** shown in *bold*), the coordination of the carboxylate group to the divalent cation is considered essential for all integrins to interact with ligands. Substitution of the Asp residue with Glu causes a loss of αvβ3 integrin-binding activity of the RGD peptide, indicating the stringency of integrin-ligand interaction (Xiong et al., 2002). More importantly, all of the integrin-ligand interfaces analyzed thus far revealed that the MIDAS cation serves as the central anchor point of integrins for their ligands (Takagi, 2007). Given the fact that the RGD motif in the ligands is indispensable for binding to RGD-binding integrins, the Arg residue, in cooperation with the Asp residue, should also contribute to the ligand recognition by RGD-binding integrins (**Figure 5C**).

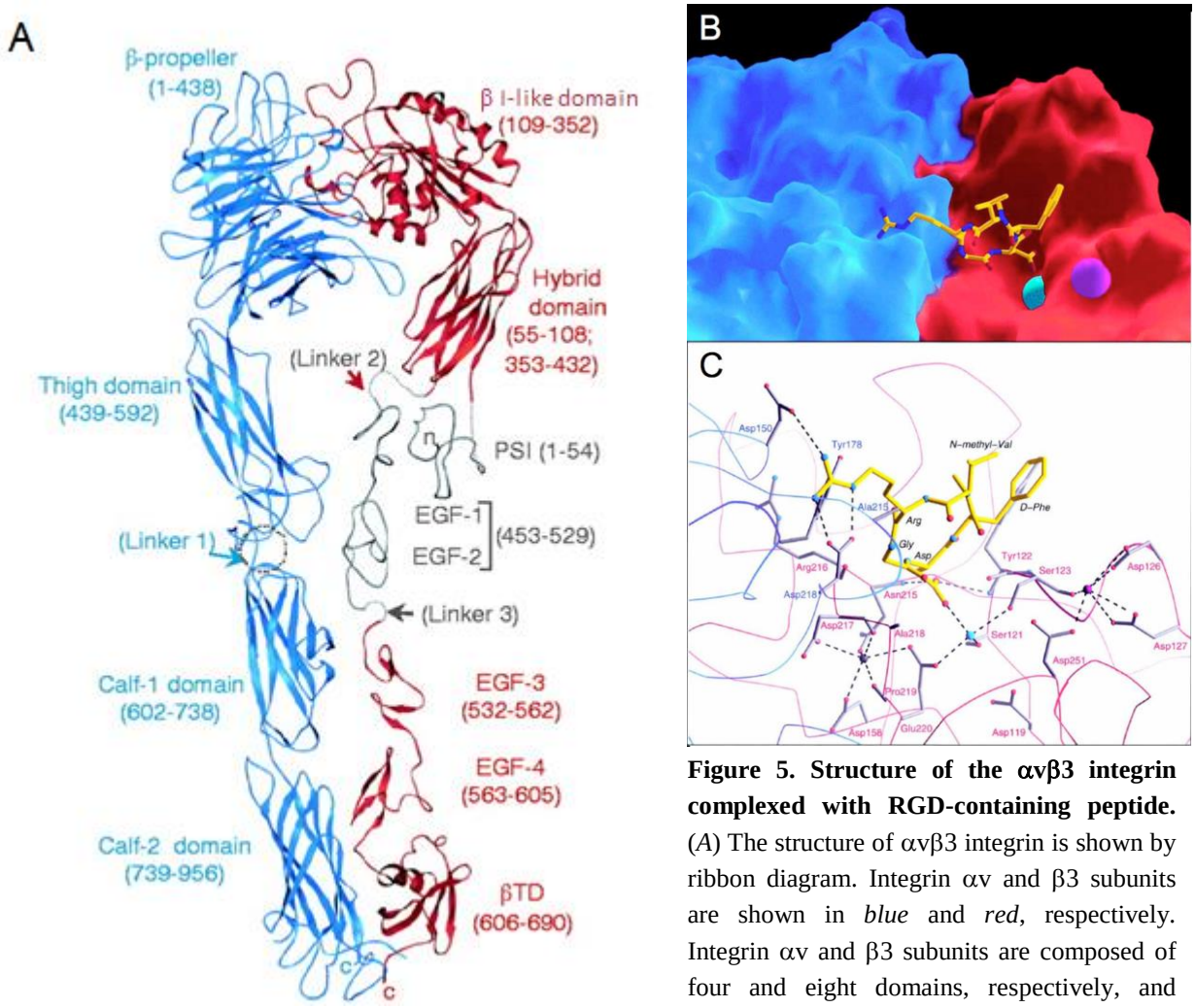

Figure 5. Structure of the αvβ3 integrin complexed with RGD-containing peptide. (*A*) The structure of αvβ3 integrin is shown by ribbon diagram. Integrin αv and β3 subunits are shown in *blue* and *red*, respectively. Integrin αv and β3 subunits are composed of four and eight domains, respectively, and strongly associate with each other at the top of the extracellular region. (*B*) Surface representation of the ligand-binding site of αvβ3 integrin, with the cyclic RGD-containing peptide shown as ball-and-stick model. The peptide ligand is bound at the β-propeller-β I-like domain interface. Manganese ions coordinated with MIDAS and adjacent to MIDAS (ADMIDAS) are represented as a *cyan* and a *violet* spheres, respectively. The carbon, nitrogen, and oxygen atoms of cyclic RGD peptide are shown in *yellow*, *blue*, and *red*, respectively. (*C*) The detail molecular mechanism of the interaction between the RGD-containing peptide and αvβ3 integrin. Polypeptides of αv and β3 subunits are simplified as *blue* and *red* line, respectively. The RGD-containing peptide is represented by *yellow* sticks. Hydrogen bonds and salt bridges are represented with dotted lines. *A* is cited from Xiong, *et al*., 2001; *B* and *C* are cited from Xiong, *et al*., 2002.

III-2. Auxiliary Sequences Required for Affinity Modulation

Although ligand recognition by RGD-binding integrins is primarily determined by the RGD motif in the ligands, several studies have demonstrated that residues outside the RGD motif define binding specificities and affinities toward individual RGD-binding integrins (Ruoslahti, 1996; Takagi, 2007) (see also **Table 2**). For example, α5β1 integrin specifically binds to fibronectin through the bipartite recognition of an RGD motif in the 10th type III

repeat, together with the PHSRN sequence and several basic residues within the 9th type III repeat, the latter serving as a "synergy site" (Aota et al., 1994; Redick et al., 2000). α8β1 integrin binds selectively to nephronectin via a bipartite interaction with the RGD motif and LFEIFEIER sequence, the latter located ~10 amino acid residues C-terminal to the RGD motif (Sato et al., 2009). The high-affinity binding of αvβ6 integrin to its ligands, foot-and-mouth disease virus and latent TGF-β1, requires the RGD motif and a LXXL/I sequence, of which the latter forms an α-helix to align the two conserved hydrophobic residues along the length of the helix (DiCara et al., 2007; Dong et al., 2014, 2017). Thus, the ligand-binding specificity of RGD-binding integrins might be defined by the bipartite recognition site comprising an RGD motif and residues flanking the RGD motif or those in neighboring domains that come into close proximity with the RGD motif in an intact ligand protein.

III-3. αv-containing Integrins

The integrin αv subunit was originally identified as a receptor for vitronectin (Pytela et al., 1985a). αv-containing integrins are classified as RGD-binding integrins and are widely expressed on many cell types, including neural crest cells, glial cells, muscle cells, osteoclasts, epithelial cells, and vascular endothelial cells during embryonic development and during angiogenesis in response to tumors (Brooks et al., 1994; Delannet et al., 1994, Hirsch et al., 1994; Drake et al., 1995; Friedlander et al., 1996; Weis and Cheresh, 2011). Mouse embryos containing a null mutation in the αv gene exhibit placental defects and intracerebral hemorrhage (**Table 1**), indicative of its important role in placentation and vasculogenesis. To date, the αv subunit has been shown to combine with five β subunits, β1, β3, β5, β6, and β8. αv-containing integrins interact with various extracellular matrix proteins and are considered to be promiscuous in that they exhibit broad binding specificity towards a wide variety of RGD proteins. For example, αvβ3 integrin is a representative αv integrin that has been shown to bind to EDIL3, fibrillin-1, fibrillin-2, fibronectin, bone sialoprotein, lactadherin, latent TGF-β1,

nephronectin, osteopontin, prothrombin, thrombonspondin-1, thrombospondin-2, and vitronectin (Andersen et al., 2000; Brandenberger et al., 2001; Hidai et al., 1998; Jovanovic et al., 2008; Lawler et al., 1988; Schurpf et al., 2012; Sun et al., 1992; Yokosaki et al., 2005). Among them, latent TGF-β1 has also been shown to bind to all of αv integrins, in particular αvβ6 and αvβ8 integrins, for its activation (Araya et al., 2006; Chen et al., 2002; Lu et al., 2002; Ludbrook et al., 2003; Mu et al., 2002; Munger et al., 1998).

IV. Interaction between αv-containing Integrins and TGF-βs

Integrin signaling and function are dependent on not only the interaction with extracellular ligands but also cross-talk with other signaling pathways, especially growth factor (GF) signaling pathways (Huveneers and Danen, 2009; Ivaska and Heino, 2010; Streuli and Akhtar, 2009). Integrins interact with various extracellular GFs (Hutchings et al., 2003; Vlahakis et al., 2007), GF binding proteins (Munger et al., 1998; Ricort, 2004), and GF receptors (Soro et al., 2008). Among GFs that cross-talk with integrins, TGF-β is one of the stimulatory effectors on integrin expression. For example, TGF-β signaling up-regulates the expressions of αvβ3, αvβ5, αvβ6 and several β1 integrins (Heino and Massague et al., 1989, Heino et al., 1989, Ignotz et al., 1989, Sheppard et al., 1992, Zambruno et al., 1995). On the other hands, many researchers reported that physical properties and biological activities of TGF-β are regulated by RGD-binding integrins (Araya et al., 2006; Chen et al., 2002; Lu et al., 2002; Ludbrook et al., 2003; Mu et al., 2002; Munger et al., 1998). Particularly, αv integrins interact with the latent form of TGF-β associated with ECM to induce the activation of the TGF-β in a unique mechanism.

IV-1. Latency and Activation of TGF-βs

TGF-β has been widely implicated as a master regulatory cytokine involved in paracrine regulation of blood vessel development, differentiation and function (Martin et al., 1995).

There are three different isoforms (TGF-β1-3) expressed in mammalian tissues; all of them function through the same receptor signaling pathways. TGF-β is secreted to extracellular space as a latent form containing a propeptide. Thus, TGF-β is synthesized initially as a long precursor consisting of a signal peptide, a propeptide, and the mature TGF-β (**Figure 6)**. After translocation into the endoplasmic reticulum, a monomeric TGF-β proprotein forms a disulfide-bonded homodimer, pro-TGF-β. Proteolytic cleavage by furin at the proprotein convertase cleavage site yields a complex in which the mature TGF-β remains noncovalently associated with the prodomain. The prodomain is sufficient to confer latency on mature TGF-β and prevents from binding to TGF-β receptors, therefore termed latency-associated peptide (LAP). LAP is required for the proper folding and dimerization of the carboxy-terminal domain of TGF-β (Gray and Mason, 1990; Walton et al., 2010) and is a binding target for integrins.

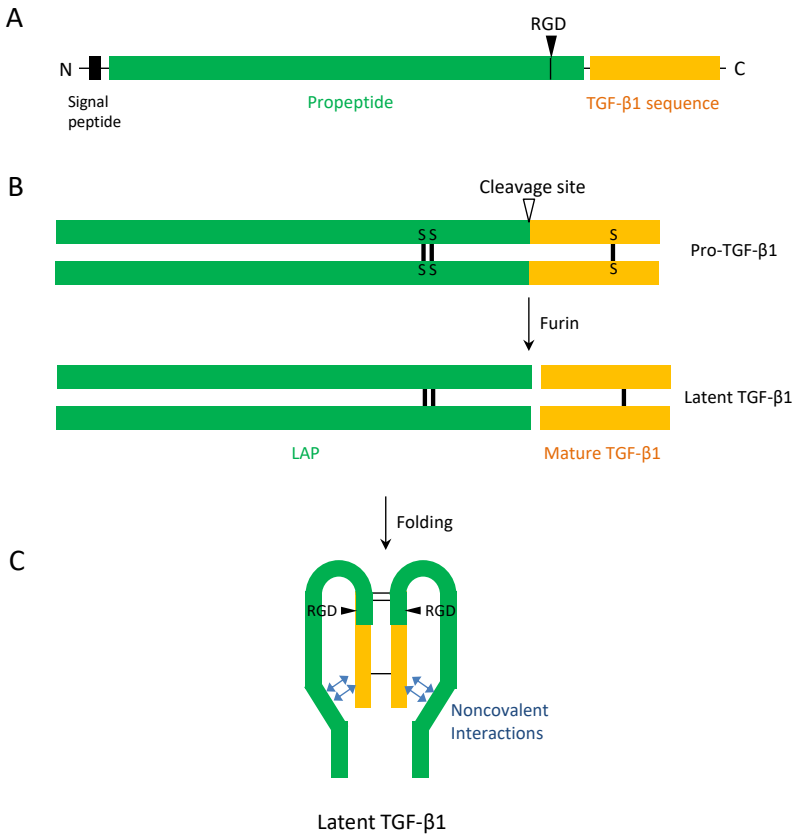

Figure 6. Structure of the latent complex form of TGF-β1. (*A*) Schematic diagram of the TGF-β1 proprotein. The propeptide region (LAP) is shown in *green*, and the TGF-β1 region in *yellow*. The *black arrowhead* indicates the positions of the RGD motif. (*B*) LAP homodimer formation. Monomeric TGF-β1 proproteins form homodimer by disulfide bonds shown in *black lines*. Proteolytic cleavage by furin creates LAP and mature TGF-β1. The *white arrowhead* indicates the position of the furin cleavage site. (*C*) Schematic diagram of latent TGF-β1. After folding, LAP and mature TGF-β1 noncovalently associates at the hydrophobic regions (*blue double-headed arrows)*. These figures were modified from Munger and Sheppard (2011), "Cross Talk among TGF-β Signaling Pathways, Integrins, and the Extracellular Matrix," in Hynes and Yamada, eds., *Extracellular Matrix Biology*, Cold Spring Harbor Laboratory Press, p. 186.

IV-2. Interaction of Latent TGF-β with αv-containing Integrins

Several factors can activate latent TGF-β (Annes et al., 2003). Plasmin and a number of matrix metalloproteinases (MMPs) are proposed to cleave LAP in integrin-independent manner, and the released TGF-β activates TGF-β signaling pathways. The LAP-TGF-β complex contains a protease-sensitive hinge region which can be the potential target for this liberation of mature TGF-β. Most of latent TGF-β activations are achieved by αv-containing integrins. LAPs of TGF-β1 and TGF-β3 contain an RGD motif that is recognized by a vast majority of αv-containing integrins, αvβ1, αvβ3, αvβ5, αvβ6 and αvβ8. (Araya et al., 2006; Chen et al., 2002; Lu et al., 2002; Ludbrook et al., 2003; Mu et al., 2002; Munger et al., 1998). The RGD sequence is highly conserved among TGF-βs in chordates, but is not present in other TGF-β superfamily members, indicating that the activation of latent TGF-β by the αv integrins is the mechanism conserved in the process of evolution.

IV-3. Redundancy among TGF-β Isoforms and αv-containing Integrins

The fact that the αv–containing integrins are physiological activators for TGF-β1 and TGF-β3 is mirrored by strong overlaps among phenotypes of TGF-β-null and integrin αv gene-null mice, as shown in **Table 3.** Mice with a knock-in mutation of TGF-β1, in which an RGD motif is mutated to nonfunctional RGE (TGF-$\beta1^{RGE/RGE}$ mice), recapitulate the major phenotype of TGF-β1-deficient mice (TGF-$\beta1^{-/-}$ mice) including multi-organ inflammation and defects in vasculogenesis, thus demonstrating the essential role of αv integrins in TGF-β1 activation during development and growth (Yang et al., 2007). Among αv integrins, αvβ6 and αvβ8 integrins appear to be largely responsible for TGF-β1 activation at least in regard to the phenotypes of TGF-β1-deficient mice. Mice with a null mutation of the gene encoding the integrin β6 subunit (Itgb6$^{-/-}$ mice) develop lymphocytic lung inflammation reminiscent of inflammation in TGF-$\beta1^{-/-}$ mice (Huang et al., 1996), suggesting a possibility that the

interaction between αvβ6 integrin and latent TGF-β1 is required for normal lung homeostasis and response to lung injury. In contrast, mice deficient in the expression of the integrin β8 subunit (Itgb8$^{-/-}$ mice) exhibit variable embryonic lethality with vasculogenesis failure and severe brain hemorrhage (Zhu et al., 2002), as is the case with mice deficient in integrin αv subunit expression (Bader et al., 1998). The phenotypes of mice lacking integrin β8 expression largely overlap with those of the mice deficient in integrin-mediated TGF-β1 activation, TGF-β1$^{RGE/RGE}$ and TGF-β3$^{-/-}$ mice (Arnold et al., 2014; Cambier et al., 2005), demonstrating the importance of TGF-β1 activation by αvβ8 integrin.

Table 3. Comparison of phenotypes of mice with TGF-β gene mutations and those lacking β6 and/or β8 integrins.

Mouse	Phenotype
Tgfb1$^{-/-}$	Variable (strain-dependent) embryonic lethality because of vasuculogenesis failure; lethal multiorgan lymphocyte-mediated inflammation and lack of Langerhans cells in remainder.
Tgfb1$^{RGE/RGE}$	Identical to Tgfb1$^{-/-}$, reduced fibrosis in heterozygotes.
Tgfb2$^{-/-}$	Embryonic lethality with defects in multiple organ systems.
Tgfb3$^{-/-}$	Cleft palate caused by failure of fusion of palatal shelves; mild, variable delayed lung development.
Itg av$^{-/-}$	~80% embryonic lethality because of vasculogenesis failure; brain hemorrhage and cleft palate in remainder. Note that these mice lack αvβ1, αvβ3, αvβ5, αvβ6, and αvβ8 integrins.
Itg β6$^{-/-}$	Lymphocyte-predominant lung inflammation, reduced Langerhans cells, late-onset lung emphysema because of increased MMP-12, reduced fibrosis.
Itg β8$^{-/-}$	Variable embryonic lethality because of vasculogenesis failure, CNS hemorrhage, cleft palate (~10%); conditional KO in dendritic cells causes mild inflammation.
Itg β6$^{-/-}$ Itg β8$^{-/-}$	Individual phenotypes plus high incidence of cleft palate causing early postnatal death.
Itg β8$^{-/-}$ treated prenatally with anti-αvβ6	Lethal multiorgan lymphocyte-mediated inflammation, lack of Langerhans cells.

This table is cited from Munger and Sheppard (2011), "Cross Talk among TGF-β Signaling Pathways, Integrins, and the Extracellular Matrix," in Hynes and Yamada, eds., *Extracellular Matrix Biology*, Cold Spring Harbor Laboratory Press, p. 194.

V. Activation of Latent TGF-β by αvβ6 and αvβ8 Integrins

The binding of αv integrins to LAP is not sufficient for TGF-β activation. Currently there are two proposed models of how αv-containing integrins activate latent TGF-β1; one model is centered on αvβ6 integrin and involves conformational change of the latent TGF-β1 complex that results in releasing the active TGF-β1; and the other model focuses on the role of αvβ8 integrin and involves protease-dependent mechanism.

V-1. αvβ6 Integrin-mediated Mechanism Underlying TGF-β Activation

αvβ6 integrin was the first integrin to be identified as latent TGF-β1 activator. αvβ6 integrin binds LAP in latent TGF-β1 and TGF-β3 complexes and alters the conformation of the complexes, effectively releasing the mature TGF-β1 (Annes et al., 2002; Munger et al., 1999). Importantly, activation of latent TGF-β1 requires the cytoplasmic domain of β6 and rearrangement of the actin cytoskeleton, suggesting that contractile forces generated by actin cytoskeleton and translated into biochemical signals are necessary for activation of latent TGF-β1 by αvβ6 integrin (**Figure 7A**). This pathway has been demonstrated for activation of TGF-β in epithelial cells and allows the active TGF-β to bind to its receptors on adjacent cells. This mechanism does not require MMPs and implies that the expression of αvβ6 integrin can locally regulate TGF-β function *in vivo*.

V-2. Protease-dependent TGF-β Activation by αvβ8 Integrin

αvβ8 integrin binds to the latent TGF-β1 and activates it by releasing mature TGF-β1 from LAP (Mu et al., 2002). αvβ8 integrin and TGF-β1 are co-expressed in human airway and perivasucular astrocytes (Cambier et al., 2005; Crawford et al., 1998). Recent study demonstrated that the β8 integrin is specifically expressed in Schwann cells to activate TGF-β1, thereby regulating hematopoietic stem cell hibernation in bone marrow (Yamazaki et al.,

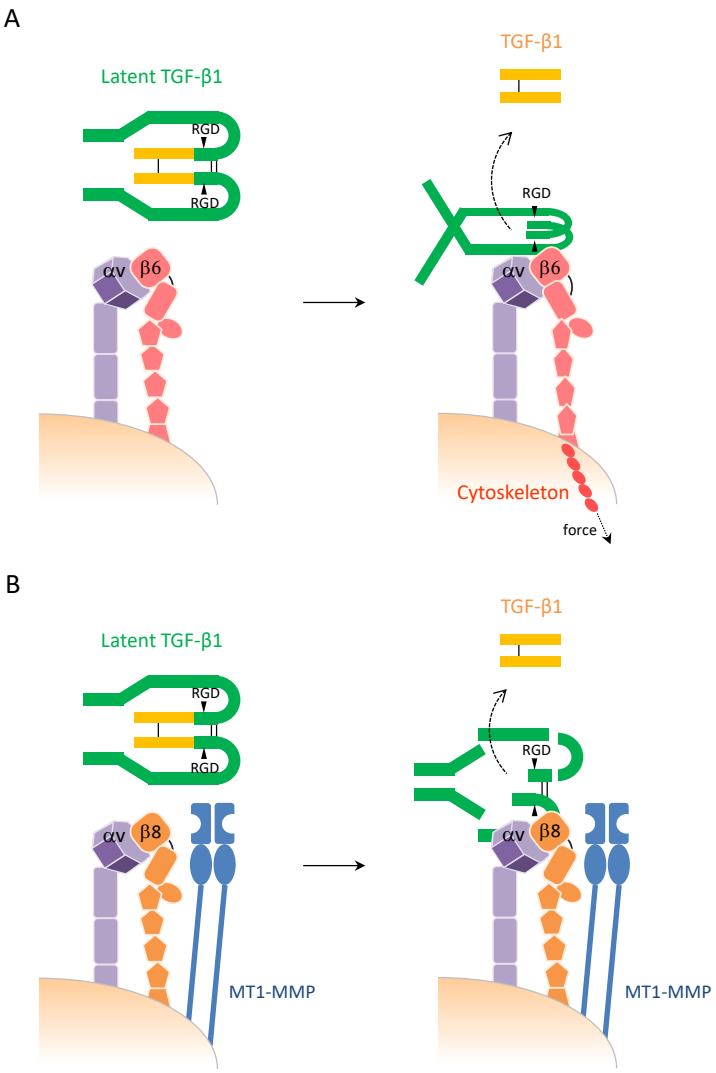

Figure 7. The proposed mechanisms underlying TGF-β activation by the αvβ6 (*A*) and αvβ8 (*B*) integrins. (*A*) To activate the latent TGF-β1, the binding of αvβ6 integrin to the RGD motif in LAP is the initial step. Then, contractile force through αvβ6 integrin, driven by rearrangement of the actin cytoskeleton, induces the conformational change of latent TGF-β1 and releases mature TGF-β1. (*B*) Activation of latent TGF-β1 by αvβ8 integrin depends on MT-MMP1, but not on actin cytoskeleton. MT-MMP1 expressed near the αvβ8 integrin at the membrane surface cleaves LAP and releases mature TGF-β1. Figures are modified from Munger *et al*., 1999; Tatti *et al*., 2008.

2011). In contrast to the TGF-β1 activation by αvβ6 integrin, which requires the β6 subunit cytoplasmic domain and a functional actin cytoskeleton, TGF-β activation by αvβ8 integrin is considered independent of the β8 subunit cytoplasmic domain and actin cytoskeleton, because cells expressing a mutated β8 subunit lacking the cytoplasmic tail can activate TGF-βs (Mu et al., 2002; Araya et al., 2006). Binding assays combined with cell adhesion studies showed that αvβ8-expressing cells release active TGF-β1 into the medium in concert with activation of MT1-MMP (Mu et al., 2002). MT1-MMP co-localizes with αvβ8 integrin at the membrane surface of cells adhering to LAP and cleaves near the N-termini of LAP (Tatti et al., 2008) (**Figure 7B**). Therefore, the role of the αvβ8 integrin is to create a close connection between the latent TGF-β and MT1-MMP.

V-3. Physiological Roles of αvβ8 Integrin

The amino acid sequence of the β8 subunit is highly conserved among vertebrates but is divergent from other integrin β subunits (Moyle et al., 1991), suggesting that αvβ8 integrin may have unique functions among the αv-containing integrins. The exogenous expression of integrin β8 inhibited cell growth, spreading, and focal contact formation (Cambier et al., 2000; Nishimura et al., 1994), in contrast to the exogenous expression of other αv-containing integrin β subunits. The β8 subunit is found in the brain, kidneys, airways, and placenta and is localized at brain vessels, synapses, glial cells, and dendritic spines, implying a specific function in the brain (Moyle et al., 1991; Nishimura et al., 1998). To date, αvβ8 integrin has been shown to bind vitronectin (Nishimura et al., 1994), fibronectin (Venstrom and Reichardt, 1995), and the LAP of TGF-β1/3 (Mu et al., 2002; Worthington et al., 2011), among which TGF-β1 is the most characterized ligand for αvβ8 integrin. However, neither the mechanism by which αvβ8 integrin interacts with TGF-β1 nor the binding capability of αvβ8 integrin to its potential ligands containing RGD motif has been comprehensively investigated by a biochemical method using purified proteins, leaving the possibility that unknown proteins containing the RGD motif may also serve as ligands that specifically interact with αvβ8 integrin.

In the present study, I comprehensively investigated the binding activities of αvβ8 integrin towards 25 RGD-containing proteins selected by *in silico* screening for putative secreted proteins containing a conserved RGD motif. Our results showed that αvβ8 integrin has a restricted binding specificity towards latent TGF-β1, which is primarily defined by the Leu-218 residue located immediately after the RGD motif. The Leu-218 residue is critical for the αvβ8 integrin-binding ability because substitution of RGDL for RGDS sequence of fibronectin results in binding of αvβ8 integrin to fibronectin. The mechanism by which αvβ8 integrin recognizes the Leu-218 residue was investigated by constructing a series of swap mutants between integrin β8 and β3 subunits.

Experimental Procedures

Cells, Antibodies, and Reagents—FreeStyle™ 293-F cells were obtained from Life Technologies (Carlsbad, CA) and cultured in FreeStyle 293-F Expression medium. Human plasma fibronectin was purified from outdated human plasma by gelatin affinity chromatography as previously described (Sekiguchi and Hakomori, 1983). HRP-conjugated mAbs against FLAG and penta-His tags were purchased from Sigma (Saint Louis, MO) and Qiagen (Valencia, CA), respectively. An anti-"Velcro" (ACID/BASE coiled-coil) antibody was raised in rabbits by immunization with coiled-coil ACID and BASE peptides as previously described (Takagi et al., 2001) and biotinylated by an Ez-link NHS-Sulfo-LC-biotin kit (Pierce, Rockford, IL) to detect recombinant integrins. HRP-conjugated streptavidin was purchased from Pierce. Synthetic peptides were purchased from Thermo Fisher Scientific (Dreieich, Germany) and dissolved in 100% DMSO.

In Silico Screening of RGD Motif-containing Proteins—The Protein Information Resource (PIR) Perfect Peptide Match program was used to screen proteins registered in the UniProt Knowledgebase (UniprotKB) (Apweiler et al., 2004; Chen et al., 2013). Non-redundant proteins possessing at least one RGD motif were selected, and then further screened for their ability to be secreted into the extracellular space, based on their annotation in the Uniprot database or the presence or absence of signal peptides and transmembrane regions, respectively, which were predicted by using PSORT II (Nakai and Horton, 1999) and SOSUI (Hirokawa et al., 1998). Conservation of RGD motifs in vertebrates was assessed using the Ensembl genome database (Hubbard et al., 2002).

cDNA Cloning and Construction of Expression Vectors—cDNA encoding human latent TGF-β1 was amplified by PCR using a latent TGF-β1 cDNA clone purchased from Life Technologies (IMAGE clone 3356605) as a template. The amplified cDNA was subcloned into pBluescript II KS+

vector (Stratagene, La Jolla, CA). After verification by DNA sequencing, the amplified cDNA was digested with *Hind*III/*Eco*RI and inserted into the corresponding restriction sites of the pSecTag2B vector (Invitrogen), yielding the latent TGF-β1 expression vector pSecTag-TGF-β1. cDNAs encoding human angiopoietin-related protein 7 (ANGPTL7, IMAGE clone 3544149), human EGF-like repeat and discoidin-I like domain-containing protein 3 (EDIL3, IMAGE clone 4791845), human osteopontin (SPP1, IMAGE clone 4284921), and human vitronectin (VTN, IMAGE clone 4040317) were obtained from the Mammalian Gene Collection and amplified by PCR using individual cDNA clones as templates. cDNAs encoding insulin-like growth factor-binding protein 2 (IGFBP2), lactadherin (MFGE8, deleted for its second discoidin-like domain), thrombospondin-1 (THBS1), thrombospondin-2 (THBS2), bone sialoprotein (IBSP), EGF-like, fibronectin type III and laminin G domains (EGFLAM), prothrombin (F2), TGF-β1-induced protein ig-h3 (BIGH3), proprotein convertase subtilisin/kexin type 6 (PCSK6), wingless-type MMTV integration site family, member 10A (WNT10A), fibrillin-1 (FBN1; a truncated form consisting of 23-28th EGF-like repeats and 6-7th TGF-β-binding (TB) domains), fibrillin-2 (FBN2; a truncated form consisting of 5th TB, 21-26th EGF-like repeats and 6th TB domains), fibulin-5 (FBLN5), netrin-1 (NTN1), and hemicentin-2 (HMCN2, a truncated form consisting of 4th and 5th immunoglobulin-like domains) were amplified by reverse transcription-PCR. Template RNAs used for PCR amplification were obtained from A549 cells (for IGFBP2 and MFGE8), HeLa-S3 cells (for THBS1 and THBS2), human fetal brain (Clontech, Palo Alto, CA; for IBSP, EGFLAM), human fetal liver (Clontech; for F2, BIGH3, PCSK6 and WNT10A), and human fetal heart (Clontech; for FBN1, FBN2, FBLN5, NTN1 and HMCN2). PCR-amplified cDNAs except for latent TGF-β1 were subcloned into pSecTag2B vector (Invitrogen) in which a FLAG tag was inserted in-frame to the Igκ leader sequence at the 5′ end and verified by DNA sequencing. A list of the primer sequences used for PCR is described in **Table 4**. A cDNA encoding human fibronectin III7-10 (FNIII7-10; a truncated form consisting of the 7-10th type-III domains) was amplified by PCR using a fibronectin cDNA clone (Manabe et al., 1997) as a template. The amplified cDNA was subcloned into the pBluescript II KS+ vector. After verification by DNA sequencing, the amplified

cDNA was digested with *Hind*III/*Pst*I and inserted into the corresponding restriction sites of the pSecTag2B vector, yielding an expression vector for FNIII7-10 designated pSecTag-FNIII7-10.

A cDNA encoding the extracellular region of human integrin β3, β6 and β8 were amplified by reverse transcription-PCR. Template RNAs used for PCR amplification were extracted from WiDr human colon carcinoma cells (for β6 and β8) and T98G human glioblastoma cells (for β5) as templates, respectively. The PCR-amplified cDNA was digested with *Bam*HI/*Pme*I and inserted into the corresponding restriction sites of the pEF expression vector in frame to the sequence encoding the "BASE" peptide and a 6xHis tag at the 3′ end of the integrin β8 cDNA as described previously (Ido et al., 2007). Another pEF vector encoding the extracellular region of integrin β8 lacking a C-terminal 6xHis tag was also constructed by overlap extension PCR for expression of recombinant αvβ8 integrin lacking the 6xHis tag [designated as αvβ8(ΔHis)]. The expression vectors for the extracellular regions of integrin αv and β3 were described previously (Ido et al., 2007; Takagi et al., 2001). cDNAs encoding a series of swap mutants of the extracellular region of integrin β8 and β3 were amplified by PCR using cDNAs encoding the integrin β8 and β3 as a template, respectively. The primer sequences for PCR are described in **Table 4**. After verification by DNA sequencing, PCR-amplified cDNA fragments were digested with *Bam*HI and *Nhe*I and inserted into the corresponding restriction sites of pEF-integrin β8-BASE-6xHis or pEF-integrin β3-BASE-6xHis and verified by DNA sequencing, respectively.

Site-directed Mutagenesis—Site-directed mutagenesis of latent TGF-β1 and a truncated form of fibronectin (FNIII7-10) was accomplished by overlap extension PCR with KOD polymerase using pSecTag-TGF-β1 and pSecTag-FNIII7-10 as templates, respectively. The primer sequences for the site-directed mutagenesis are available upon request. After verification by DNA sequencing, the PCR products containing the mutations were subcloned into pSecTag2B vector.

Expression and Purification of Recombinant Proteins and Integrins—GST-fused EGF-like protein 6 (EGFL6), GST-fused FRAS-1 related extracellular matrix protein 1 (FREM1), laminin-α5 (LAMA5, as laminin-511), and nephronectin (NPNT) were purified as described previously (Ido et al., 2004; Kiyozumi et al., 2005; Osada et al., 2005; Sato et al., 2009; Sekiguchi and Hakomori, 1983). For purification of other RGD-containing proteins, FreeStyle 293-F cells (Life Technologies) were transiently transfected with individual expression vectors according to the manufacturer's instructions. The conditioned media were collected at 72 h after transfection and centrifuged to remove cells and debris, followed by addition of Pefabloc SC (Roche, Basel, Switzerland; 0.4 mM), imidazole (10 mM), and sodium azide (0.02%). The conditioned media were incubated with nickel-nitrilotriacetic acid-agarose (Ni-NTA) beads (Qiagen), followed by washing with TBS. Bound proteins were eluted with TBS containing 200 mM imidazole. The eluted fractions except for latent TGF-β1, vitronectin, thrombospondin-1, and PCSK6 were applied to columns of anti-FLAG M2 agarose beads (Sigma), and the bound proteins were eluted with 100 μg/mL FLAG peptide (Sigma). Recombinant latent TGF-β1, vitronectin, thrombospondin-1, and PCSK6 were purified by one-step Ni-NTA affinity chromatography. The purified proteins were dialyzed against TBS and quantified by a Bio-Rad Protein Assay kit (Bio-Rad, Hercules, CA) using bovine serum albumin (BSA) as a standard. Recombinant integrins were expressed in FreeStyle 293-F cells by cotransfection with expression vectors encoding integrin α and β subunits, and purified as described above by two-step affinity chromatography, except for αvβ8(ΔHis), which was purified by one-step chromatography using anti-FLAG-M2 agarose.

SDS-PAGE and Western Blotting—SDS-PAGE was carried out according to Laemmli (Laemmli, 1970) using 8, 12, or 5–20% gradient gels. Separated proteins were visualized by Coomassie Brilliant Blue (CBB) staining or transferred onto PVDF membranes (Millipore, Billerica, MA) for immunoblotting. The membranes were treated with TBS containing 5% skim milk and 0.05% Tween-20 for detection of FLAG tags or anti-His blocking reagent (Qiagen) containing 0.05% Tween-20 for detection of 6xHis tags. The membranes were then probed with HRP-conjugated

antibodies against FLAG or penta-His tags, followed by visualization with the ECL Western blotting substrate (GE Healthcare).

Integrin Binding Assay—Integrin binding assays were performed as described previously (Nishiuchi et al., 2006). Briefly, microtiter plates (Nunc-Immuno™ MicroWell™ 96-well plates; Thermo Fisher Scientific) were coated with various RGD-containing proteins (10 nM) overnight at 4°C, and then blocked with TBS containing 10 mg/mL BSA. The plates were incubated with integrins in the presence of 1 mM $MnCl_2$ with or without 10 mM EDTA. In inhibition assays, integrins were incubated on the plates in the presence of synthetic peptides at various concentrations to evaluate their inhibitory activities. The plates were washed with TBS containing 1 mM $MnCl_2$, 0.1% BSA, and 0.02% Tween-20 with or without 10 mM EDTA, followed by quantification of bound integrins by an ELISA using a biotinylated rabbit anti-Velcro antibody and HRP-conjugated streptavidin. Integrin binding assays were also performed in a reverse manner. Briefly, microtiter plates were coated with 10 nM αvβ8(ΔHis) integrin and then incubated with various RGD-containing proteins having a 6xHis tag. Bound proteins were quantified by ELISA using an HRP-conjugated anti-penta-His antibody. The results represent the means of triplicate determinations. Apparent dissociation constants were calculated by saturation binding assays as described previously (Nishiuchi et al., 2006).

Table 4. PCR primer sequences

Protein names	Primer types	Sequences	Restriction sites	
			5'end	3'end
Latent TGF-β1	Forward	5'-AAGCTTCATCATCATCATCATGGACTATCCACCTGCAAGAC-3'	HindIII	EcoRI
	Reverse	5'-AAAGAATTCTCAGCTGCACTTGCAGGAGCGCAC-3'		
ANGPTL7	Forward	5'-AAAGAATTCCAGAAGCTCTCTAAGCACAAGACACCAGCACAG-3'	EcoRI	XhoI
	Reverse	5'-AAACTCGAGAGGCTTGAAGTCTTCTGGGCGGATTTTCATC-3'		
BIGH3	Forward	5'-AAAAAGCTTGGTCCCGCCAAGTCGCCCTACCAGCTGGTGCTG-3'	HindIII	XhoI
	Reverse	5'-AAACTCGAGAATGCTTCATCCTCTCTAATAACTTTTGATAG-3'		
EDIL3	Forward	5'-AAAAAGCTTGTCCCCCAGTTCGGCAAAGGTGATATTTG-3'	HindIII	BamHI
	Reverse	5'-AAAGGATCCTTCCTCCTCTGTGCAGCCCAGCAGCTC-3'		
EGFLAM	Forward	5'-AAAAAGCTTCTCCGAGCGGCCATCCGAAAACCAGGCAAGG-3'	HindIII	XhoI
	Reverse	5'-AAACTCGAGACTTGGCTCCACAAGTGTTGATGTTTTTCCC-3'		
FBLN5	Forward	5'-TTTAAGCTTCAGGCACAGTGCACGAATG-3'	HindIII	XhoI
	Reverse	5'-TTTCTCGAGTGAATGGGTACTGCGACAC-3'		
Fibrillin-1	Forward	5'-AAAGGTACCGATCTGGACGAATGTTCCAATGG-3'	KpnI	EcoRI
	Reverse	5'-AAAGAATTCCTTGACTTCCACAGAGTGTAGCAAAC-3'		
Fibrillin-2	Forward	5'-CCCGGTACCGATGTCAATGAATGTGACCTAAATTC-3'	KpnI	EcoRI
	Reverse	5'-AAAGAATTCCGCCTTCACCTCCGGGACAC-3'		
HMCN2	Forward	5'-AAAAAGCTTCATGCGCCCCAGCTG-3'	HindIII	PstI
	Reverse	5'-AAACTGCAGCACCTGGACCACCAG-3'		
IBSP	Forward	5'-AAAAAGCTTTTCTCAATGAAAAATTTGCATCGAAGAGTC-3'	HindIII	XhoI
	Reverse	5'-AAACTCGAGACTGGTGGTGGTAGTAATTCTGACCATCATAG-3'		
IGFBP2	Forward	5'-TTTCTCGAGTAATATCTCTGCATTCGTACTTGAGG-3'	HindIII	XhoI
	Reverse	5'-TTTCTCGAGTAATATCTCTGCATTCGTACTTGAGG-3'		
MFGE8	Forward	5'-CCCAAGCTTCTGGATATCTGTTCCAAAAACCCC-3'	HindIII	XhoI
	Reverse	5'-TTTCTCGAGTTCCGTTCAGCTCACAGCCC-3'		
NTN1	Forward	5'-AAAGGTACCGGGCCCGGGCTCAGC-3'	KpnI	EcoRI
	Reverse	5'-AAAGAATTCCGGCCTTCTTGCACTTGCCC-3'		
Osteopontin	Forward	5'-AAAAAGCTTATACCAGTTAAACAGGCTGATTCTGGAAGTTCTG-3'	HindIII	BamHI
	Reverse	5'-AAAGGATCCATTGACCTCAGAAGATGCACTATCTAATTCATGAG-3'		
PCSK6	Forward	5'-AAAGGATCCCCCCCGCCGCGCCCCGTCTACACCAACCAC-3'	BamHI	NotI
	Reverse	5'-AAAGCGGCCGCCCCGGCCAGGAGGCACGTGCGGCAG-3'		

Prothrombin	Forward	5’-AAAGGTACCGGCAACCTGGAGCGAGAG-3’	KpnI	EcoRI
	Reverse	5’-AAAGAATTCCCTCTCCAAACTGATCAATGACC-3’		
Thrombospondin-1	Forward	5’-CCCAAGCTTAACCGCATTCCAGAGTCTGGC-3’	HindIII	XhoI
	Reverse	5’-TTTCTCGAGTGGGATCTCTACATTCGTATTTCAGGTC-3’		
Thrombospondin-2	Forward	5’-CCCAAGCTTGGTCACCAGGACAAAGACAC-3’	HindIII	XhoI
	Reverse	5’-TTTCTCGAGTAATATCTCTGCATTCGTACTTGAGG-3’		
Vitronectin	Forward	5’-AAAAAGCTTGACCAAGAGTCATGCAAGGGC-3’	HindIII	PstI
	Reverse	5’-GGCTGCAGCAGATGGCCAGGAGC-3’		
WNT10A	Forward	5’-AAAGGATCCATGCCCAGGTCAGCACCCAATGACATTCTG-3’	BamHI	XhoI
	Reverse	5’-AAACTCGAGACTTGCAGACGCTGACCCACTCGGTGATG-3’		
β8 integrin	Forward	5’-GGATCCGAATTTCTCCATCCAAG-3’	BamHI	PmeI
	Reverse	5’-GCGGCCGCTTTGTAGCCAAACATG-3’		
β5 integrin	Forward	5’-GGATCCGCTGAGGGAGGCGCCC-3’	BamHI	PmeI
	Reverse	5’-GCGGCCGCTCAATGGTGATGGTGATG-3’		
β6 integrin	Forward	5’-GGATCCGAAACGACCACCATGG-3’	BamHI	PmeI
	Reverse	5’-GCGGCCGCTCAATGGTGATGGTG-3’		

Results

I. In Silico Screening of RGD-containing Proteins as Candidates for αv Integrin Ligands—Among the currently available databases for protein sequences, UniProtKB is a suitable resource for the screening of putative αv integrin ligands because it contains ~91,800 human protein sequences, some of which are manually annotated with information extracted from the literature (**Figure 8**). I performed protein sequence-based screening for proteins containing an RGD motif using the Protein Information Resource Perfect Peptide Match program and extracted 5,083 proteins containing at least one RGD sequence. Given that this program often assigns different ID numbers for alternatively spliced variants and/or fragments, I reassigned the same ID numbers for such variants, thus yielding a non-redundant protein list comprising 1,909 proteins possessing at least one RGD motif. Because integrins are cell-surface receptors that recognize extracellular proteins, I next screened for putative secreted proteins based on the annotation of UniProtKB or the presence of a signal peptide and the absence of transmembrane region(s), respectively, as predicted by PSORTII and SOSUI. This yielded 190 putative secreted proteins with an RGD motif. Because integrin αv is evolutionarily conserved among vertebrates, I assumed that the ligands for αv integrins should have an RGD motif conserved among vertebrates. Screening of 190 putative secreted proteins among vertebrate orthologs that harbored the conserved RGD motif yielded 29 candidates for αv integrin ligands (**Table 5**).

II. Recombinant Expression and Purification of the Candidates for αvβ8 Integrin Ligands—I expressed and purified the 29 RGD-containing proteins listed in **Table 5**. Fibronectin, EGF-like protein 6 (EGFL6), FREM1, laminin-α5 (LAMA5, as laminin-511), and nephronectin were purified as described previously (Ido et al., 2004; Kiyozumi et al., 2005;

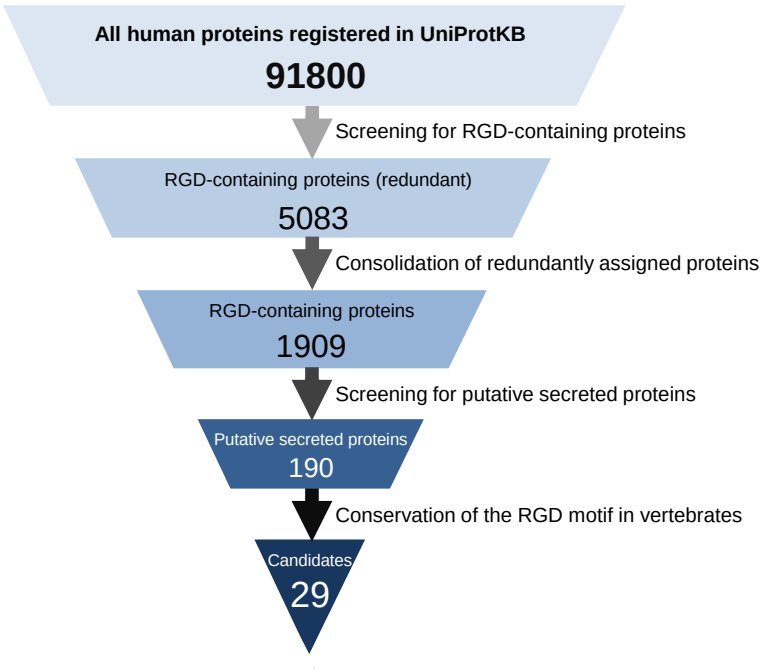

Figure 8. *In silico* screening of RGD-containing secreted proteins. All human proteins registered in UniProtKB were screened for putative αv integrin ligands based on the following three criteria: 1) possession of an RGD motif(s), 2) secretion to the extracellular space, and 3) conservation of the RGD motif among vertebrates. For details, see the text and *Experimental Procedures*. The final list comprising 29 candidate proteins for αv integrin ligands is shown in **Table 5**.

Osada et al., 2005; Sato et al., 2009; Sekiguchi and Hakomori, 1983). Latent TGF-β1 was expressed as a recombinant protein using a mammalian expression system with a 6xHis tag at the N-terminus and purified from conditioned medium by Ni-NTA affinity chromatography. Other proteins were expressed with N-terminal FLAG and C-terminal 6xHis tags to ensure the secretion of full-length proteins. Secreted recombinant proteins were purified from the conditioned medium by Ni-NTA affinity chromatography. When protein purity was not sufficient, they were further purified by anti-FLAG mAb affinity chromatography. The authenticity of the purified proteins was verified by SDS-PAGE under reducing conditions, followed by CBB staining and immunoblotting against the FLAG and 6xHis tags. Purified latent TGF-β1 gave three bands migrating at 50 kDa (unprocessed latent TGF-β1), 37 kDa (LAP), and 10 kDa (mature TGF-β1) (**Figure 9A**), confirming the authenticity of the purified protein (Dubois et al., 1995). Except for thrombospondin-1, proprotein convertase subtilisin/kexin type 6 (PCSK6), semaphorin-3C (SEMA3C), extracellular matrix protein 2 (ECM2), lysine-tRNA synthetase (KARS), and PCSK5, the other proteins were also purified at their mass regions (**Figure 9B**). Thrombospondin-1 and PCSK6 were obtained as

Table 5. Candidate proteins for αvβ8 integrin ligands.

Gene symbols	Protein names	N-tag	C-tag	Purification methods
ANGPTL7	angiopoietin-related protein 7	FLAG	His	Ni-NTA & anti-FLAG
BIGH3	transforming growth factor-β induced protein ig-h3	FLAG	His	Ni-NTA & anti-FLAG
ECM2[c]	extracellular matrix protein 2	FLAG	His	Ni-NTA & anti-FLAG
EDIL3	EGF-like repeat and discoidin l-like domain containing protein 3	FLAG	His	Ni-NTA & anti-FLAG
EGFL6	EGF-like protein 6	GST	-	(Osada et al., 2005)
EGFLAM	EGF-like, fibronectin type III and laminin G domains (pikachurin)	FLAG	His	Ni-NTA & anti-FLAG
F2	Prothrombin	FLAG	His	Ni-NTA & anti-FLAG
FBLN5	fibulin-5	FLAG	His	Ni-NTA & anti-FLAG
FBN1[b]	fibrillin-1	FLAG	His	Ni-NTA & anti-FLAG
FBN2[b]	fibrillin-2	FLAG	His	Ni-NTA & anti-FLAG
FINC[a]	fibronectin[a]	-	-	(Sekiguchi and Hakomori, 1983)
FREM1	FRAS1-related extracellular matrix protein 1	GST	-	(Kiyozumi et al., 2005)
HMCN2[b]	hemicentin-2	FLAG	His	Ni-NTA & anti-FLAG
IBSP	bone sialoprotein 2	FLAG	His	Ni-NTA & anti-FLAG
IGFBP2	insulin-like growth factor-binding protein 2	FLAG	His	Ni-NTA & anti-FLAG
KARS[c]	lysine-tRNA ligase	FLAG	His	Ni-NTA & anti-FLAG
LAMA5	laminin α5 subunit	-	-	(Ido et al., 2004)
MFGE8[b]	lactadherin	FLAG	His	Ni-NTA & anti-FLAG
NPNT	nephronectin	-	FLAG	(Sato et al., 2009)
NTN1	netrin-1	FLAG	His	Ni-NTA & anti-FLAG
PCSK5[c]	proprotein convertase subtilisin/kexin type 5	FLAG	His	Ni-NTA & anti-FLAG
PCSK6[b]	proprotein convertase subtilisin/kexin type 6	FLAG	His	Ni-NTA
SPP1	osteopontin	FLAG	His	Ni-NTA & anti-FLAG
SEMA3C[c]	semaphorin-3C	FLAG	His	Ni-NTA & anti-FLAG
TGFB1[a]	transforming growth factor-β1[a]	His	-	Ni-NTA
THBS1[b]	thrombospondin-1	FLAG	His	Ni-NTA
THBS2	thrombospondin-2	FLAG	His	Ni-NTA & anti-FLAG
VTN[a]	vitronectin[a]	FLAG	His	Ni-NTA
WNT10A	wingless-type MMTV integration site family, member 10A	FLAG	His	Ni-NTA & anti-FLAG

[a] Known αvβ8 ligands.

[b] Candidate proteins that were purified as truncated forms.

[c] Candidate proteins that could not be purified because of low expression.

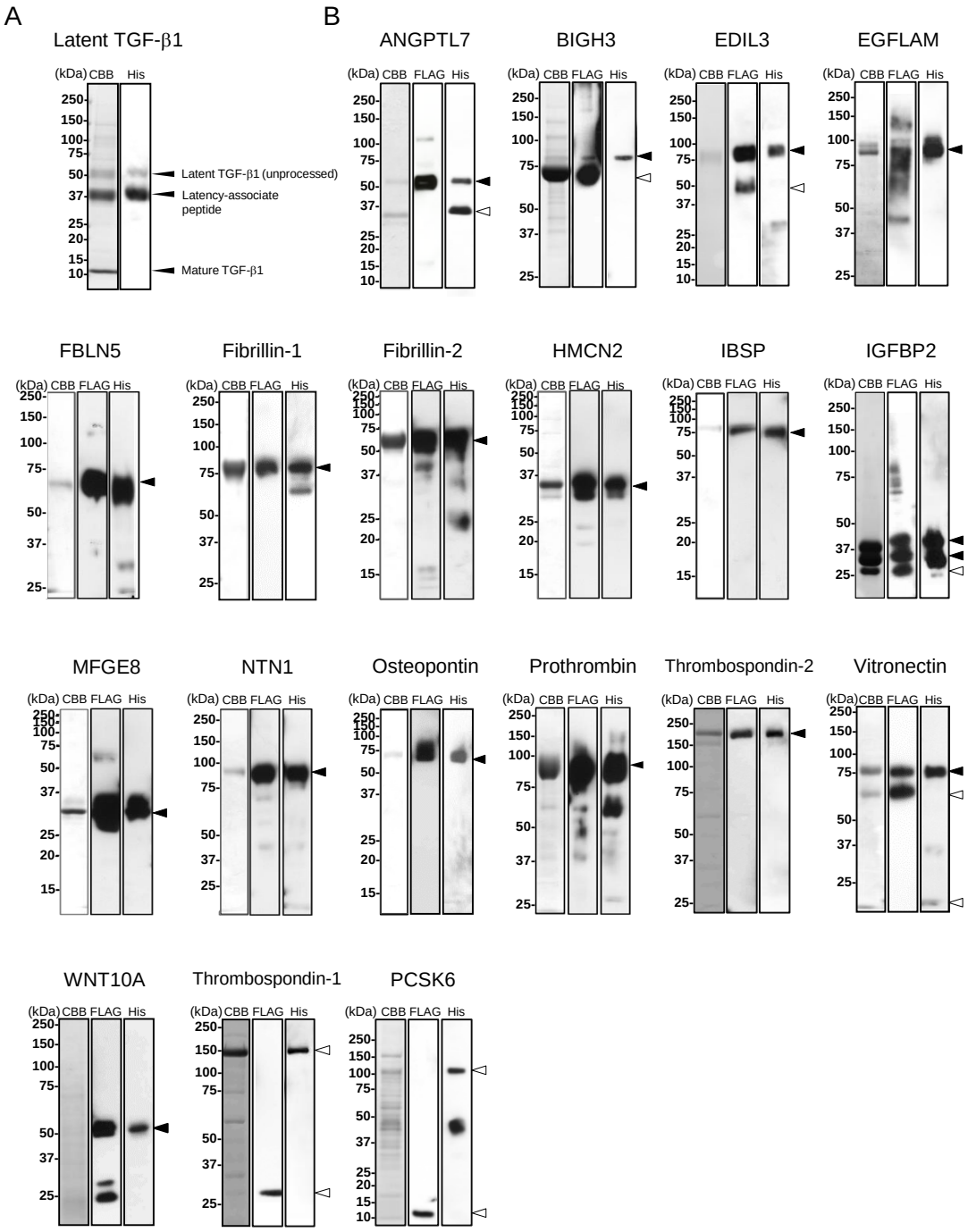

Figure 9. Purification of recombinant RGD proteins. Purified latent TGF-β1 (*A*) and other recombinant RGD proteins (*B*) were subjected to SDS-PAGE on 5–20% gradient gels (ANGPTL7, EDIL3, PCSK6, and latent TGF-β1), 8% gels (EGFLAM, BIGH3, FBLN5, IGFBP2, NTN1, prothrombin, thrombospondin-2, vitronectin, WNT10A, and thrombospondin-1) or 12% gels (fibrillin-1, fibrillin-2, HMCN2, IBSP, MFGE8, and osteopontin) under reducing conditions, followed by CBB staining (left), immunoblotting with an anti-FLAG monoclonal antibody (middle), or with an anti-penta His monoclonal antibody (right). Molecular masses are indicated on the left of panels. Arrowheads indicate predicted molecular size of full-length (*close*) or processed form (*open*) of each recombinant protein.

proteolytically processed forms comprising N- and C-terminal fragments by Ni-NTA affinity chromatography. It was difficult to obtain sufficient amounts of recombinant SEMA3C, ECM2, KARS, and PCSK5 for subsequent integrin binding assays because of their low levels of expression and/or proteolytic degradation.

III. Binding Activities of αv Integrins toward 25 RGD-containing Proteins—αv-containing integrins are comprised of five closely related isoforms, namely αvβ1, αvβ3, αvβ5, αvβ6 and αvβ8, which are considered to be promiscuous in that they exhibit broad binding specificity towards a wide variety of RGD proteins. To compare the ligand binding capabilities of αv integrins, a total of 25 RGD proteins (hereafter designated as "RGD proteins") were purified and subjected to integrin binding assays using recombinant αv integrins. αv integrins were expressed and purified as disulfide-linked heterodimers of the extracellular domains of αv and individual β chains. I excluded αvβ1 integrin from comprehensive integrin binding assays because of its low level of expression. The purified four αv integrins including αvβ8, αvβ3, αvβ5 and αvβ6 gave a single band migrating at ~250 kDa upon SDS-PAGE under non-reducing conditions and were resolved into four bands, *i.e.* ~150 kDa (unprocessed αv chain), ~120 kDa (αv heavy chain), ~100 kDa (β chain), and ~30 kDa (αv light chain), under reducing conditions, respectively (**Figure 10**).

The integrin binding assays were performed in the presence of 1 mM Mn^{2+} to fully activate integrins. Comprehensive binding assays showed that four αv integrins displayed a distinct binding specificity toward a broad range of RGD proteins, although they share the same integrin αv subunit (**Figure 11**). αvβ8 integrin strongly bound to latent TGF-β1, but it also bound to other RGD proteins moderately (fibrillin-1, fibrillin-2, fibronectin, and vitronectin) or only marginally (EDIL3, bone sialoprotein (IBSP), and osteopontin).

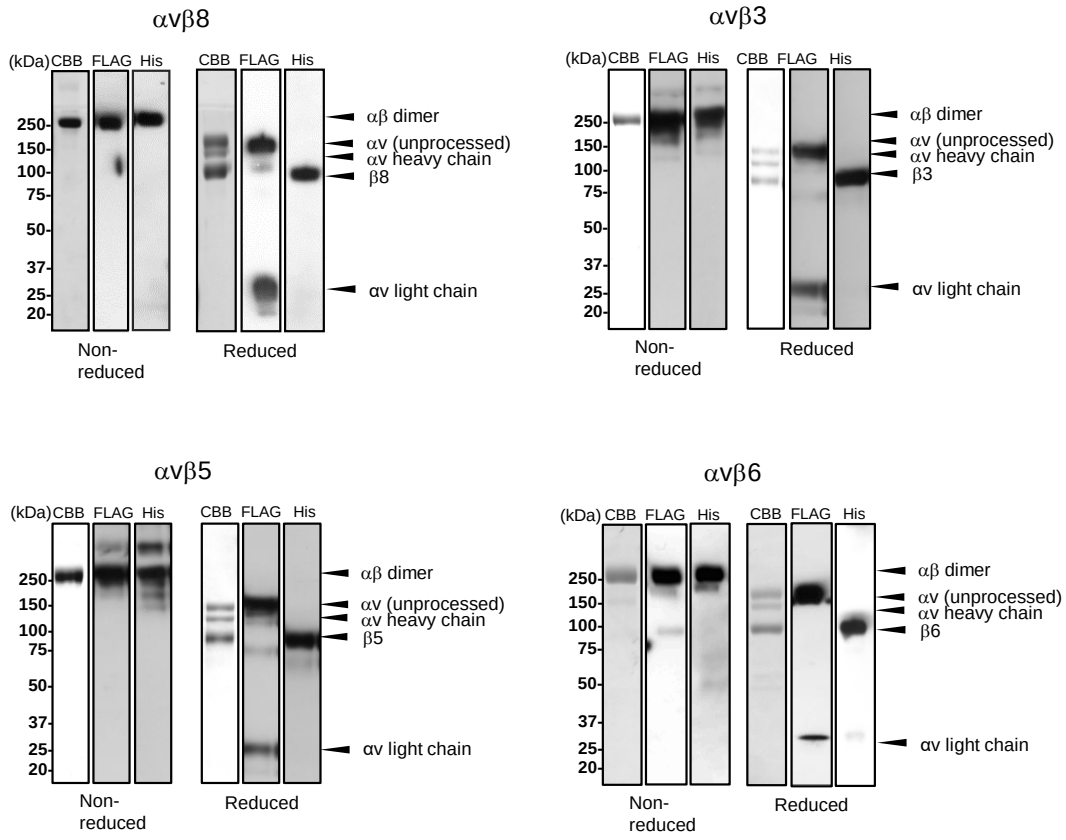

Figure 10. Purification of recombinant αvβ8, αvβ3, αvβ5 and αvβ6 integrins. Purified αv integrins were subjected to SDS-PAGE on 5–20% gradient gels under reducing or non-reducing conditions, followed by CBB staining (left), immunoblotting with an anti-FLAG monoclonal antibody (middle), or with an anti-penta His monoclonal antibody (right). Molecular masses are indicated on the left of panels. Arrowheads indicate predicted molecular size of full-length or processed form of each αv integrins.

In contrast, αvβ3 integrin bound strongly to EDIL3, fibrillin-1, fibrillin-2, fibronectin, IBSP, and vitronectin, moderately to EGFL6, FREM1, laminin α5, lactadherin (MFGE8), and osteopontin, but had low binding affinity for EGFLAM, fibulin-5 (FBLN5), nephronectin, prothrombin, latent TGF-β1, thrombospondin-1, and thrombospondin-2. The binding specificity of αvβ5 integrin was remarkably similar to that of αvβ3 integrin; αvβ5 integrin strongly bound to EDIL3, fibrillin-1, fibrillin-2, IBSP, laminin α5, and vitronectin, moderately to EGFL6, EGFLAM, fibronectin, FREM1, MFGE8, nephronectin, osteopontin and PCSK6 but had low binding affinity for fibulin-5, prothrombin, latent TGF-β1, thrombospondin-1, and thrombospondin-2. αvβ6 integrin also exhibited a broad spectrum of binding affinity toward

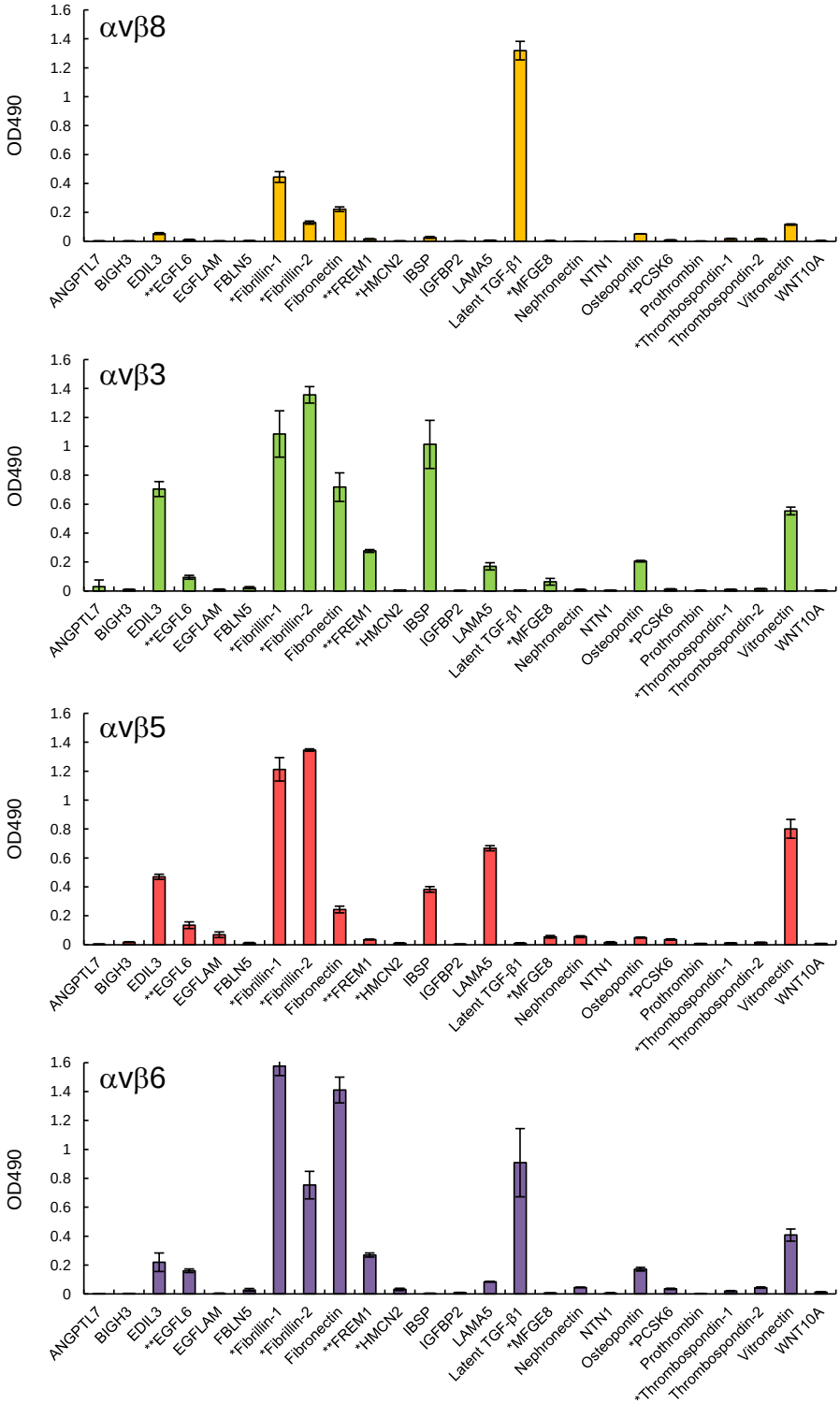

Figure 11. Binding activities of αv integrins towards 25 RGD proteins. Microtiter plates were coated with RGD proteins (10 nM) and then incubated with individual αv integrins (10 nM) in the presence of 1 mM Mn^{2+}. The bound integrins were quantified using a biotinylated anti-Velcro polyclonal antibody and HRP-conjugated streptavidin as described in the *Experimental Procedures*. The amounts of integrin bound in the presence of 10 mM EDTA were used as negative controls, and subtracted as backgrounds. The results represent the means ± S.D. of triplicate determinations. *Candidate proteins expressed as fragments containing an RGD motif. **Candidate proteins expressed as recombinant fragments fused to GST at their N-termini.

25 RGD proteins, spectrum of binding affinity toward 25 RGD proteins, but it slightly differed from αvβ3 and αvβ5 integrins in its binding specificity; αvβ6 integrin bound strongly to fibrillin-1, fibrillin-2, fibronectin and latent TGF-β1, moderately to EDIL3, EGFL6, FREM1, laminin α5, osteopontin and vitronectin, but only marginal binding activities were observed toward the other RGD proteins. Consistent with these results, EDIL3, fibrillin-1, fibrillin-2, fibronectin, IBSP, MFGE8, latent TGF-β1, nephronectin, osteopontin and vitronectin have been shown to interact with individual αv-containing integrins (Andersen et al., 2000; Brandenberger et al., 2001; Hidai et al., 1998; Jovanovic et al., 2008; Lawler et al., 1988; Schurpf et al., 2012; Sun et al., 1992; Yokosaki et al., 2005). These results indicated that the αvβ8 integrin has a highly restricted ligand specificity to TGF-β1 and significantly differs from other αv integrins in ligand binding specificity.

IV. αvβ8 Integrin Preferentially Binds to Latent TGF-β1—Among the 25 RGD proteins I examined, latent TGF-β1 was extremely potent in binding to αvβ8 integrin, and EDIL3, fibrillin-1, fibrillin-2, fibronectin, osteopontin, and vitronectin were moderately active, while other RGD proteins did not show any significant binding to αvβ8 integrin (**Figure 11**). Because the coating efficiency varies among the 25 RGD proteins, I also performed reverse binding assays in which microtiter plates were coated with αvβ8 integrin without a 6xHis tag and then incubated with a panel of RGD proteins added in the solution phase. Bound RGD proteins were detected with an HRP-conjugated anti-penta-His antibody. EGFL6, fibronectin, FREM1, laminin-α5, and nephronectin, all of which did not possess a 6xHis tag, were not included in this assay. Among the 20 RGD proteins tested, only latent TGF-β1 bound strongly to αvβ8 integrin in a divalent cation-dependent manner (**Figure 12A**). ANGPTL7 and IBSP also gave positive signals in the assay, but the signals persisted in the presence of 10 mM EDTA, suggesting that they did not represent authentic interactions of αvβ8 integrin with its

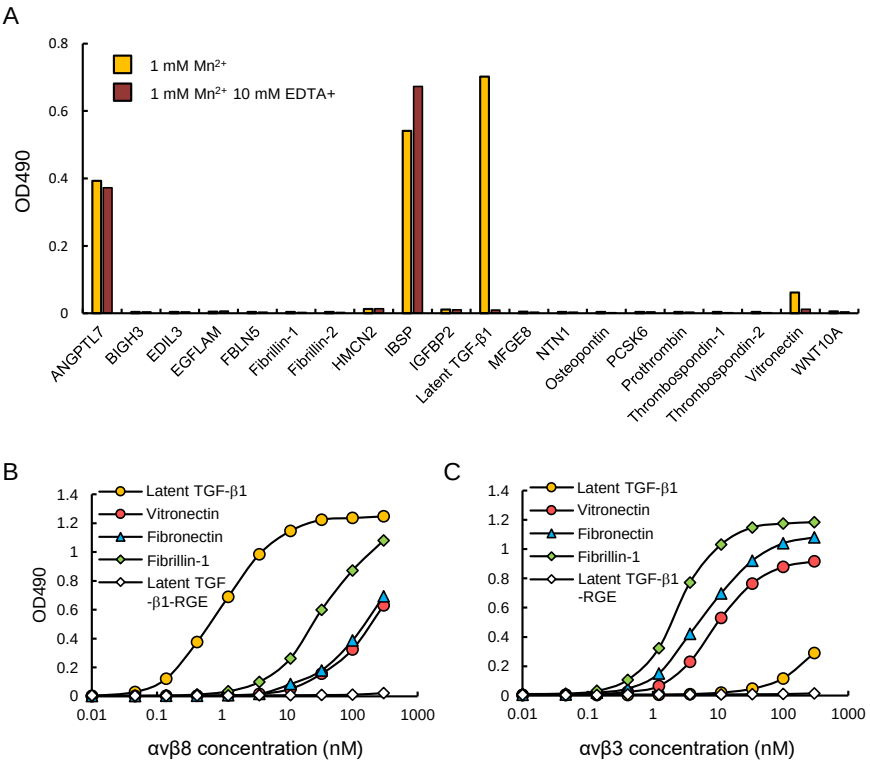

Figure 12. Ligand binding specificity of αvβ8 integrin. (*A*) Binding activities of αvβ8 integrin toward 20 RGD proteins in the solution phase. Microtiter plates were coated with αvβ8(ΔHis) integrin (10 nM) and then incubated with RGD proteins (10 nM) in the presence of 1 mM Mn^{2+} or 10 mM EDTA. The bound RGD proteins were quantified using an HRP-conjugated anti-6xHis antibody as described in the *Experimental Procedures*. (*B* and *C*) Titration curves of αvβ8 (*left*) and αvβ3 (*right*) integrins bound to latent TGF-β1 (*yellow circles*), vitronectin (*red circles)*, fibronectin (*blue triangles*), fibrillin-1 (*green diamonds*), and the RGD→RGE substitution mutant of latent TGF-β1 (*white diamonds*). The results represent the means of three independent determinations. Bound integrins were quantified as described in the *Experimental Procedures*.

ligand through the divalent cation in the β8 subunit. The results obtained in two separate assays of the reverse format indicated that αvβ8 integrin preferentially bound to latent TGF-β1 with an affinity far exceeding those to fibronectin and vitronectin, the known ligands for αvβ8 integrin. Saturation binding assays revealed that αvβ8 integrin bound to latent TGF-β1 with an apparent dissociation constant of 2.3 ± 0.2 nM, which was approximately one or two orders of magnitude lower than that of fibrillin-1, fibronectin, and vitronectin (**Figure 12B**). Substitution of the RGD motif of latent TGF-β1 with an inactive RGE sequence completely abrogated the ability of latent TGF-β1 to bind to αvβ8 integrin, confirming the RGD-dependent interaction of latent TGF-β1 with αvβ8 integrin. The low binding affinities of αvβ8 towards vitronectin, fibronectin, and fibrillin-1 were not caused by inactivation of their RGD ligand activity because they retained the ability to bind to αvβ3 integrin, an integrin that binds to these RGD proteins (**Figure 12C**). It should be noted that αvβ3 integrin showed only marginal binding

activity to latent TGF-β1. Its activity was nullified by substitution of the RGD motif with an inactive RGE sequence (**Figure 12C**). These results indicated that the ligand specificity and binding affinity of αvβ8 integrin towards latent TGF-β1 differ significantly from αvβ3 integrin.

V. Leu-218 Residue Immediately Following the RGD Motif is Required for High-affinity Binding to αvβ8 Integrin—To explore the molecular basis of the restricted ligand specificity of αvβ8 integrin, I focused on the LXXI sequence immediately following the RGD motif, because the LXXI sequence was required for the high-affinity binding of latent TGF-β1 to αvβ6 integrin in concert with the RGD motif (DiCara et al., 2007; Dong et al., 2014, 2017). I constructed latent TGF-β1 mutants, in which the Leu-218 and/or Ile-221 residues of the LXXI sequence were substituted with Ala and assessed their ability to bind to αvβ8 integrin (**Figure 13A**). Although the I221A substitution did not affect the binding of latent TGF-β1 to αvβ8 integrin, the L218A substitution almost completely abrogated the binding, similar to an RGD→RGE substitution (**Figure 13B**). L218A/I221A double substitution also inactivated binding to αvβ8 integrin. Dong et al. (2014) showed that the Leu residue immediately after the RGD motif of latent TGF-β3 binds to a hydrophobic pocket in the β6 subunit. However, the substitution of Leu-218 residue with Ile or Met, amino acids having larger hydrophobic side chains, also resulted in a marked loss of the ability to bind to αvβ8 integrin by latent TGF-β1 (**Figure 13C**). These results indicated that both the RGD motif and the Leu-218 residue were strictly required for the high-affinity binding of latent TGF-β1 to αvβ8 integrin.

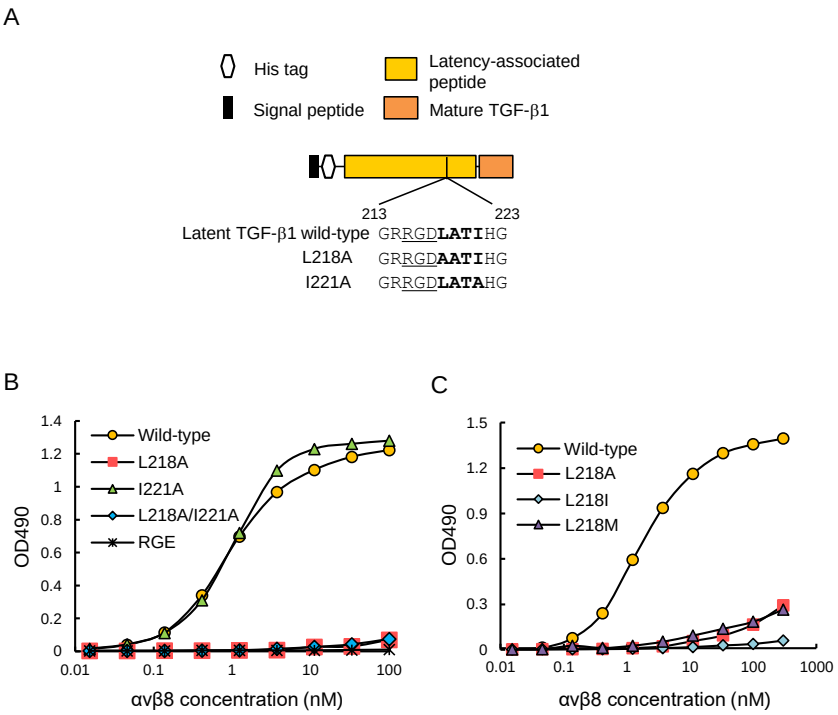

Figure 13. Effect of alanine substitutions within the LATI sequence on αvβ8 integrin-binding activity to latent TGF-β1. (*A*) Schematic of full-length TGF-β1 and the amino acid sequences of wild-type and alanine substitution mutants of latent TGF-β1. RGD motifs are *underlined*, and the following LATI sequences are shown in *bold*. (*B* and *C*) Titration curves of αvβ8 integrin bound to latent TGF-β1 (wild-type, *orange circles*), L218A substitution mutant (L218A, *red squares*), I221A substitution mutant (I221A, *green triangles*), L218A/I221A double substitution mutant (L218A/I221A, *blue diamonds*), RGD→RGE mutant (RGE, *asterisks*), L218I substitution mutant (L218I, *green diamonds*) and L218M substitution mutant (L218M, *purple triangles*). The assays were performed as described in the Figure 12 legend. The results represent the means of three independent determinations.

To confirm the importance of Leu-218 immediately following the RGD motif in latent TGF-β1 binding by αvβ8 integrin, I examined whether synthetic peptides modeled after the RGDL-containing sequence in latent TGF-β1 could inhibit the binding of latent TGF-β1 to αvβ8 integrin. I synthesized a 9-mer peptide containing the RGDL sequence (RRGDLATIH, designated as RGDL) and its mutant forms with RGDL→RGDA, RGDL→RGEL, and RGDL→RGEA substitutions (**Figure 14A**), and examined their inhibitory effects on the binding of αvβ8 integrin to latent TGF-β1. The RGDL peptide strongly inhibited the binding of αvβ8 integrin to latent TGF-β1 with an IC_{50} of ~0.3 μM (**Figure 14B and Table 6**). Substitution of the Leu residue with Ala resulted in a ~60-fold decrease in the potency of the peptide to inhibit the αvβ8 integrin-latent TGF-β1 interaction, while the RGEL peptide, in which the Asp residue of the RGD motif was substituted with Glu, resulted in a ~500-fold decrease. The RGEA peptide showed little inhibitory effect at the highest peptide concentration

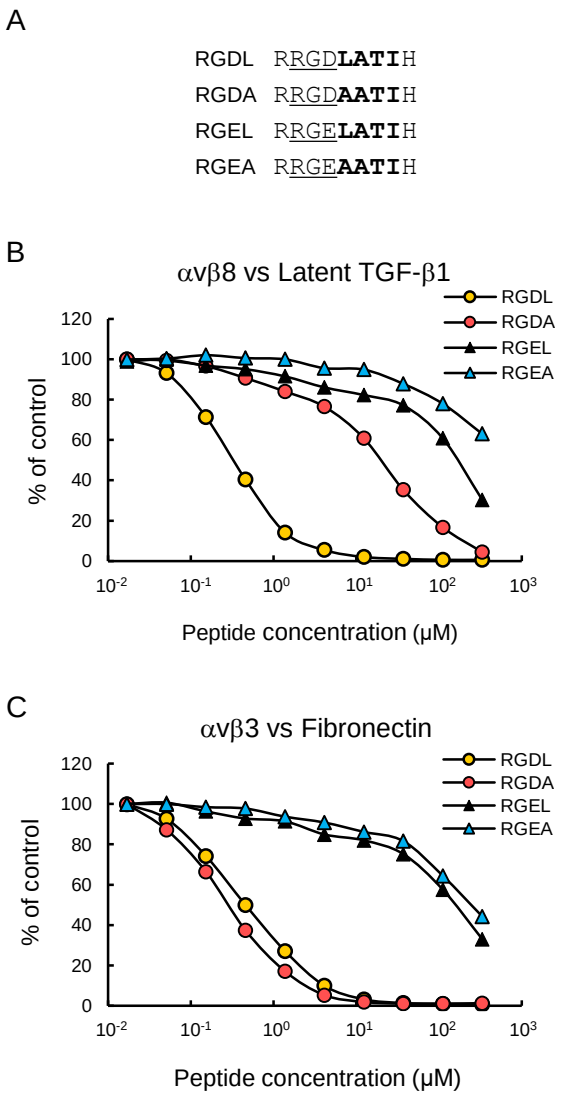

Figure 14. Inhibition of αvβ8 integrin binding to latent TGF-β1 by synthetic peptides. (*A*) Amino acid sequences of the synthetic peptides tested. RGD motifs are *underlined*, and the following LATI sequences are shown in *bold*. (*B* and *C*) Integrins (10 nM) were incubated on microtiter plates coated with latent TGF-β1 (10 nM; *B*) or fibronectin (10 nM; *C*) in the presence of increasing concentrations of synthetic peptides. To prevent precipitation of the peptides, the integrin binding assays were performed in the presence of 10% DMSO. The amounts of bound integrins are shown as percentages relative to the control, in which integrins were incubated on latent TGF-β1- or fibronectin-coated plates in the presence of 10% DMSO. The results represent the means of three independent determinations. *Yellow circles*, RGDL (9-mer containing both RGD motif and Leu residue); *red circles*, RGDA (9-mer with the Leu→Ala substitution); *black triangles*, RGEL (9-mer with RGD→RGE substitution); *blue triangles*, RGEA (9-mer with RGDL→RGEA double substitution).

used. These results indicated that although the RGD motif is the primary determinant, the Leu residue immediately after the RGD motif is critically required for the binding of αvβ8 integrin to latent TGF-β1. I also examined the potency of the peptides to inhibit the binding of αvβ3 integrin to fibronectin (**Figure 14C**). Both the RGDL and RGDA peptides were equally inhibitory with an IC_{50} of 0.3-0.4 μM, regardless of the presence or absence of the Leu residue following the RGD motif, while RGEL and RGEA peptides were only weakly inhibitory. These results indicated that the Leu residue immediately after the RGD motif is not involved in ligand recognition by αvβ3 integrin, while it is indispensable for latent TGF-β1 recognition by αvβ8 integrin.

Table 6. Inhibition of αvβ8 and αvβ3 integrin binding to ligands by synthetic peptides

integrin vs ligand	Peptides	IC50 (μM)*
αvβ8 vs latent TGF-β1	RGDL	0.31 ± 0.03
	RGDA	19 ± 1
	RGEL	170 ± 60
	RGEA	ND
αvβ3 vs fibronectin	RGDL	0.40 ± 0.10
	RGDA	0.29 ± 0.04
	RGEL	170 ± 30
	RGEA	220 ± 30

*Determined based on data from Figure 14.
The values represent the mean ± S.D. of three independent determinations.
ND, not determined.

To further corroborate the critical role of Leu-218 immediately after the RGD motif in latent TGF-β1 recognition by αvβ8 integrin, I examined whether the high-affinity binding of latent TGF-β1 toward αvβ8 integrin could be conferred on fibronectin by substituting the RGDL sequence for the RGDS cell-adhesive motif in the 10th FNIII domain of fibronectin. I produced a truncated form of fibronectin consisting of the 7-10th type III domains (FNIII7-10) and its mutants with substitution of its RGDS sequence with RGDL or RGEL and assessed their abilities to bind to αvβ8 integrin (**Figure 15A**). Although control FNIII7-10 bound to αvβ8 integrin with only a moderate affinity, the RGDL mutant bound strongly to αvβ8 integrin with an apparent Kd of 2.2 nM, which was comparable with that of latent TGF-β1 (**Figure 15B**). Substitution with the RGEL sequence completely abrogated the ability of FNIII7-10 to bind to αvβ8 integrin, underscoring the prerequisite role of the RGD motif in ligand recognition by αvβ8 integrin. These results provide further support for a critical role of the Leu residue immediately after the RGD motif in high-affinity binding of αvβ8 integrin to its ligands.

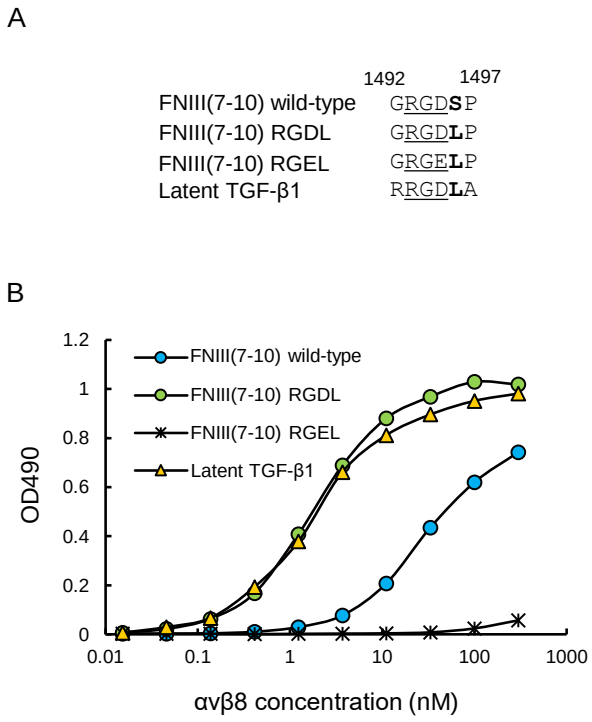

Figure 15. Effect of leucine substitution for the serine residue immediately after the RGD motif in the 10th FNIII domain of fibronectin on its αvβ8 integrin binding activity. (*A*) Amino acid sequences of wild-type and leucine-substituted mutants of FNIII7-10. RGD motifs are *underlined* and the subsequent residues are shown in *bold*. (*B*) Titration curves of αvβ8 integrin bound to wild-type FNIII7-10 (*blue circles*), RGDL mutant (*green circles*) RGEL mutant (*asterisks*), and latent TGF-β1 (*yellow triangles*). The assays were performed as described in the Figure 12 legend. The results represent the means of three independent determinations.

Dong et al. (2014) reported the crystal structure of αvβ6 integrin complexed with a latent TGF-β3 peptide containing the RGD and LXXL sequences, of which the latter forms an amphipathic α-helical structure and confers high-affinity binding of αvβ6 integrin to latent TGF-β3. To address whether the α-helical structure following the RGD motif may present the RGD motif in a conformation favorable for binding to αvβ8 integrin, I produced latent TGF-β1 mutants, in which proline was substituted for Ala-219, Thr-220, and Ile-221, respectively, to disrupt the α-helical structure following the RGD motif (**Figure 16**). Although the A219P substitution diminished the ability of latent TGF-β1 to bind to αvβ8 integrin, the T220P and I221P substitutions had no significant impact on integrin binding, suggesting that it is Leu-218 but not the proposed α-helical structure following the RGD motif that defines the specific recognition of latent TGF-β1 by αvβ8 integrin.

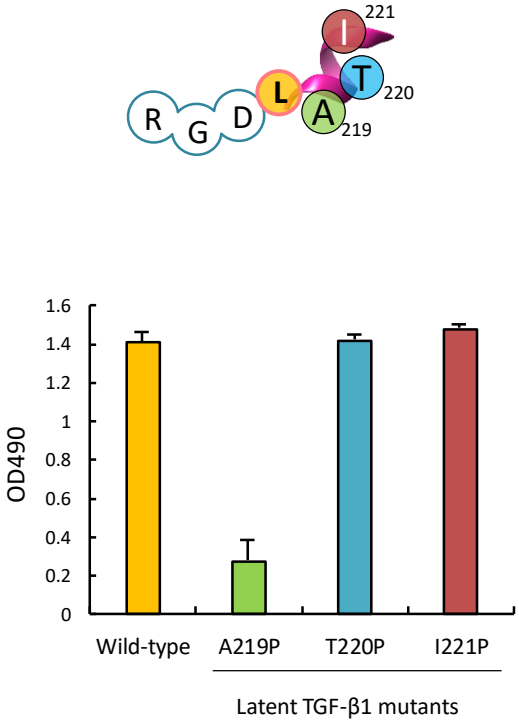

Figure 16. Effect of proline substitutions within the LATI sequence on αvβ8 integrin binding activity of latent TGF-β1. (*top*) Schematic of the RGD motif and the putative α-helical structure of LATI sequence of latent TGF-β1. (*bottom*) Binding activities of proline substitution mutants of latent TGF-β1 towards αvβ8 integrin. Wild-type, *orange*; A219P substitution mutant (A219P), *green*; T220P substitution mutant (T220P), *cyan*; I221P substitution mutant (I221P), *dark red*. The assays were performed as described in the Figure 11 legend. The results represent the means of three independent determinations.

VI. β8 I-like Domain Defines the Binding Specificity of αvβ8 Integrin to Latent TGF-β1—Given that the αvβ8 and αvβ3 integrins share the same αv subunit, the β8 subunit should be responsible for preferential recognition of latent TGF-β1 by the αvβ8 integrin. To explore the region within the β8 subunit that defines the ligand binding specificity of αvβ8 integrin, I focused on the β I-like and hybrid domains of the β8 subunit, because accumulating evidence suggests that these domains are directly involved in ligand recognition by αvβ3 and αIIbβ3 integrins (Cheng et al., 2013; Xiao et al., 2004; Xiong et al., 2002). Since that the αvβ3 integrin lacks the ability to bind to latent TGF-β1, I produced a mutant of αvβ3 integrin, designated αvβ3-8BI/HYB, in which the β3 I-like and hybrid domains were swapped with those of the β8 subunit (**Figure 17**) and assessed its binding activities towards latent TGF-β1, fibronectin, vitronectin, and fibrillin-1. Although wild-type αvβ3 integrin showed weak binding to latent TGF-β1, the αvβ3-8BI/HYB mutant exhibited strong binding, recapitulating the high-affinity binding of αvβ8 integrin to latent TGF-β1 (**Figure 18A**). In contrast, the binding activities toward fibronectin, vitronectin, and fibrillin-1 were abrogated in αvβ3-8BI/HYB, demonstrating that ligand binding specificity of αvβ8 integrin was conferred

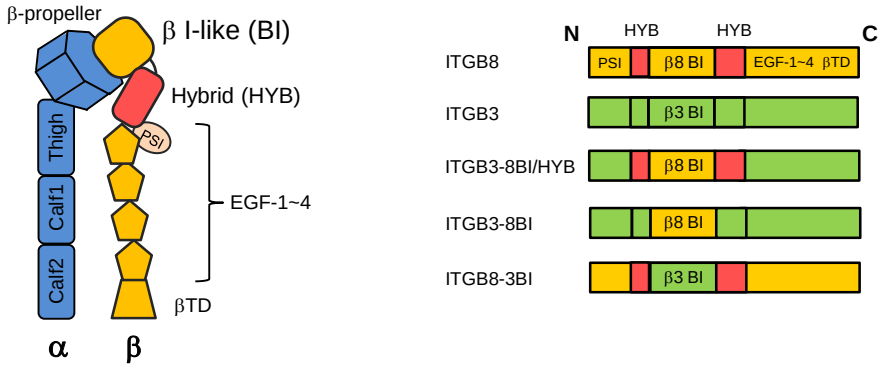

Figure 17. Schematic of the ectodomain of integrin (*left*) and representations of the β8/β3 swap mutants (*right*). The β8- and β3-derived domains are represented by *yellow boxes* and *green boxes*, respectively. The β8 hybrid domain is represented by *red boxes*.

to αvβ3 integrin by swapping the β I-like and hybrid domains. Saturation binding assays revealed that the binding affinity of the αvβ3-8BI/HYB mutant towards latent TGF-β1 was similar to that of wild-type αvβ8 integrin, yielding an apparent dissociation constant of 3.3 ± 0.5 nM (**Figure 18B and Table 7**). These results indicated that the ligand specificity and binding affinity of αvβ8 integrin to latent TGF-β1 is defined by the β8 I-like and hybrid domains.

To identify further the region responsible for latent TGF-β1 binding by αvβ8 integrin, I constructed another swap mutant of αvβ3 integrin, αvβ3-8BI, in which only the β3 I-like domain was swapped with the β8 I-like domain (**Figure 17**). The binding specificity towards latent TGF-β1 was retained by the αvβ3-8BI mutant, although its binding activity was lower than for the αvβ8 integrin and αvβ3-8BI/HYB mutants (**Figure 18A**). The apparent dissociation constant of the αvβ3-8BI mutant for latent TGF-β1 was 18 ± 1 nM (**Table 7**), demonstrating that the binding affinity towards latent TGF-β1 was approximately 6-fold lower than those of αvβ8 integrin and αvβ3-8BI/HYB. These results indicated that the β8 I-like domain primarily defines the ligand specificity of αvβ8 integrin, while the β8 hybrid domain potentiates the binding affinity towards latent TGF-β1. Consistent with these results, αvβ8-3BI, a mutant of αvβ8 integrin whose β I-like domain was swapped with the β3 I-like domain, lost

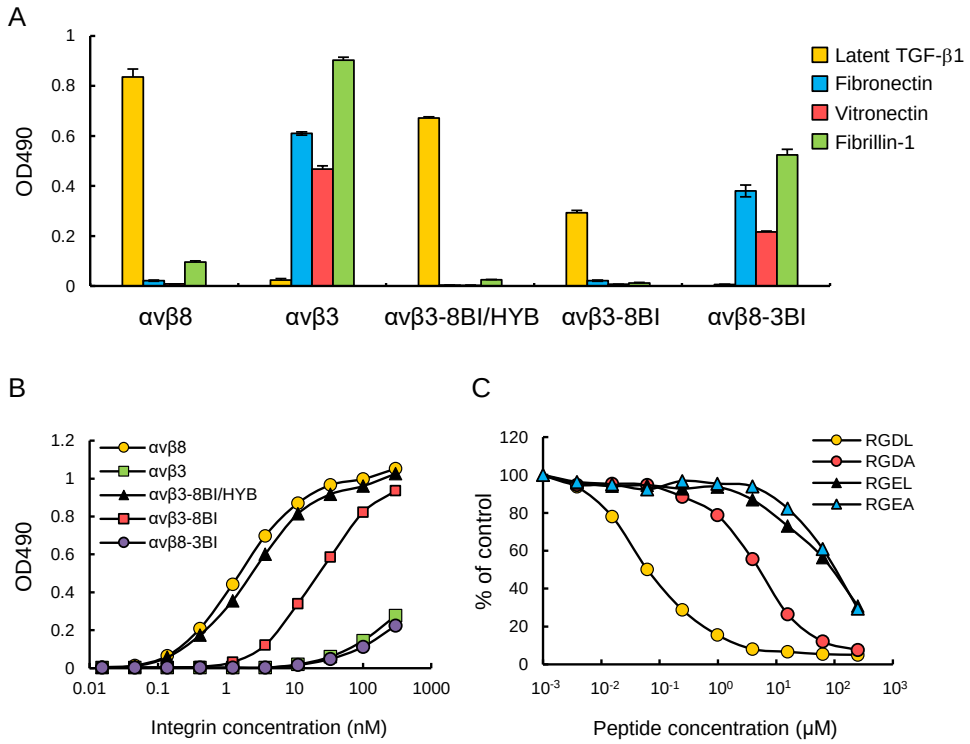

Figure 18. Ligand binding specificities of domain swap mutants of αvβ8 and αvβ3 integrins. (*A*) Binding activities of domain swap mutants of αvβ8 and αvβ3 integrins towards latent TGF-β1, fibronectin, vitronectin, and fibrillin-1. The results represent the means of three independent determinations. (*B*) Titration curves of swap mutants bound to latent TGF-β1. Increasing concentrations of αvβ8 integrin (*yellow circles*), αvβ3 integrin (*green squares*), αvβ3-8BI/HYB (*black triangles*), αvβ3-8BI (*red squares*), and αvβ8-3BI (*purple circles*) were allowed to bind to microtiter plates coated with latent TGF-β1 in the presence of 1 mM $MnCl_2$. Bound integrins were quantified as described in the *Experimental Procedures*. Apparent dissociation constants of recombinant integrins are summarized in Table 7. (*C*) Inhibition of αvβ3-8BI binding to latent TGF-β1 by synthetic peptides. The assays were performed as described in the Figure 14 legend. *Yellow circles*, RGDL (9-mer containing both RGD motif and Leu residue); *red circles*, RGDA (9-mer with the Leu→Ala substitution); *black triangles*, RGEL (9-mer with RGD→RGE substitution); *blue triangles*, RGEA (9-mer with RGDL→RGEA double substitution).

Table 7. Dissociation constants of αvβ8 integrin and its swap mutants towards latent TGF-β1.

β-chains	Kd (nM)*
β8	2.3 ± 0.2
β3	ND
β3-8BI/HYB	3.3 ± 0.5
β3-8BI	18 ± 1
β8-3BI	ND

*Values represent the mean ± S.D. of three independent experiments.
ND, not determined. The dissociation constant was not determined because of the partial saturation only being evaluated at the highest integrin concentration.

the ability to bind to latent TGF-β1 but bound avidly to fibronectin, vitronectin, and fibrillin-1 (**Figure 18A**), recapitulating the ligand specificity of wild-type αvβ3 integrin. The binding of αvβ3-8BI to latent TGF-β1 was strongly inhibited by RGDL peptide with an IC_{50} of ~0.07 μM, while substitution of the Leu residue with Ala resulted in a ~60-fold decrease in the inhibitory potency of the peptide (**Figure 18C and Table 8**). These results indicated that the β I-like domains primarily determine the binding specificity of αv-containing integrins and that the β8 I-like domain recognizes the Leu residue following the RGD motif and is necessary for the high-affinity binding of αvβ8 integrin to latent TGF-β1.

Table 8. Inhibition of ligand binding of swap mutants between αvβ3 and αvβ8 integrins by synthetic peptides

integrin vs ligand	Peptides	IC50 (μM)*
αvβ3-8BI vs latent TGF-β1	RGDL	0.07 ± 0.01
	RGDA	3.9 ± 0.9
	RGEL	32 ± 3
	RGEA	63 ± 29

*Determined based on data from Figure 18. The values represent the mean ± S.D. of three independent determinations.

VII. Role of the Disulfide-linked Loop in Latent TGF-β1 Recognition by αv Integrins—To identify the integrin β8 subunit region involved in latent TGF-β1 binding further, I focused on a small disulfide-linked loop consisting of 6–8 amino acid residues that resides on the top of the β I-like domain, designated as the "disulfide-linked loop (DLL)" (**Figure 19**). The DLL was reported to determine the ligand-binding specificities of αvβ1 and αvβ3 integrins (Takagi et al., 1997b). To address the role of the β8 subunit DLL (β8-DLL) in latent TGF-β1 recognition by αvβ8 integrin, I produced a swap mutant of αvβ3 integrin termed αvβ3-8DLL, in which the β3-DLL was swapped with the corresponding residues of the

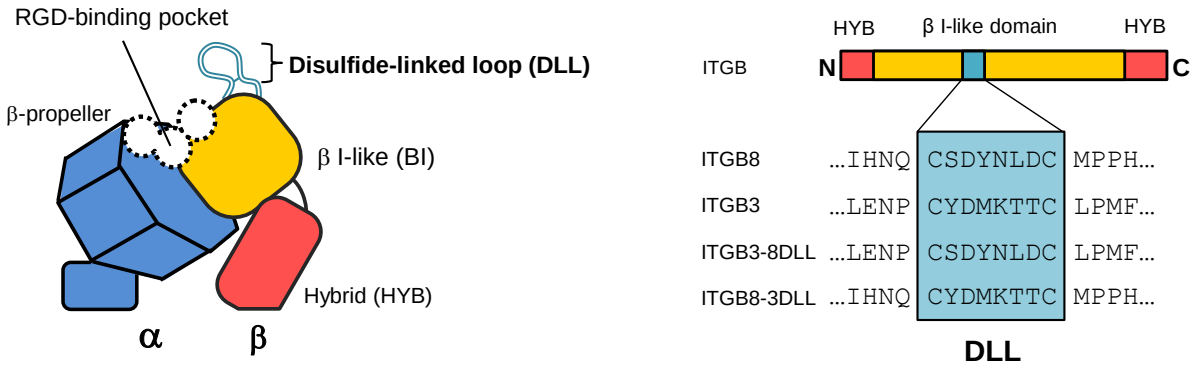

Figure 19. Schematic of the head region of integrin (*left*) and amino acid sequences of the DLL regions of the β8 and β3 subunits and their swap mutants (*right*). Swapped amino acids between the β8 and β3 subunits are indicated in the *boxed area*.

β8 subunit. The αvβ3-8DLL mutant exhibited binding to latent TGF-β1 while retaining the ability of αvβ3 integrin to bind to fibronectin, vitronectin, and fibrillin-1 (**Figure 20A**). A saturation binding assay demonstrated that the binding affinity of αvβ3-8DLL to latent TGF-β1 was significantly lower than that of wild-type αvβ8 integrin, while the affinity towards fibronectin and vitronectin was only slightly affected (**Figure 20B and Table 9**). These results indicated that β8-DLL confers latent TGF-β1 binding activity to αvβ3 integrin without compromising the ability of αvβ3 integrin to bind to its cognate ligands. I also produced another swap mutant, αvβ8-3DLL, in which the β8-DLL was swapped with the β3-DLL. Unexpectedly, the overall binding specificity of αvβ8 integrin remained unaltered after DLL swapping; αvβ8-3DLL selectively bound to latent TGF-β1 without acquiring the ability to bind to fibronectin, vitronectin, and fibrillin-1 (**Figure 20A**). Saturation binding assays indicated only a small decrease in the binding affinity towards latent TGF-β1 with αvβ8-3DLL (**Figure 20B**). Consistent with these results, the binding affinities of αvβ8-3DLL towards fibronectin and vitronectin were also unchanged after DLL swapping. These results indicated that DLL is not the primary determinant for ligand specificity of αvβ8 integrin, although it conferred latent TGF-β1 binding activity to αvβ3 integrin upon DLL swapping. It is puzzling, therefore, why β8-DLL, which is dispensable for defining the ligand specificity of

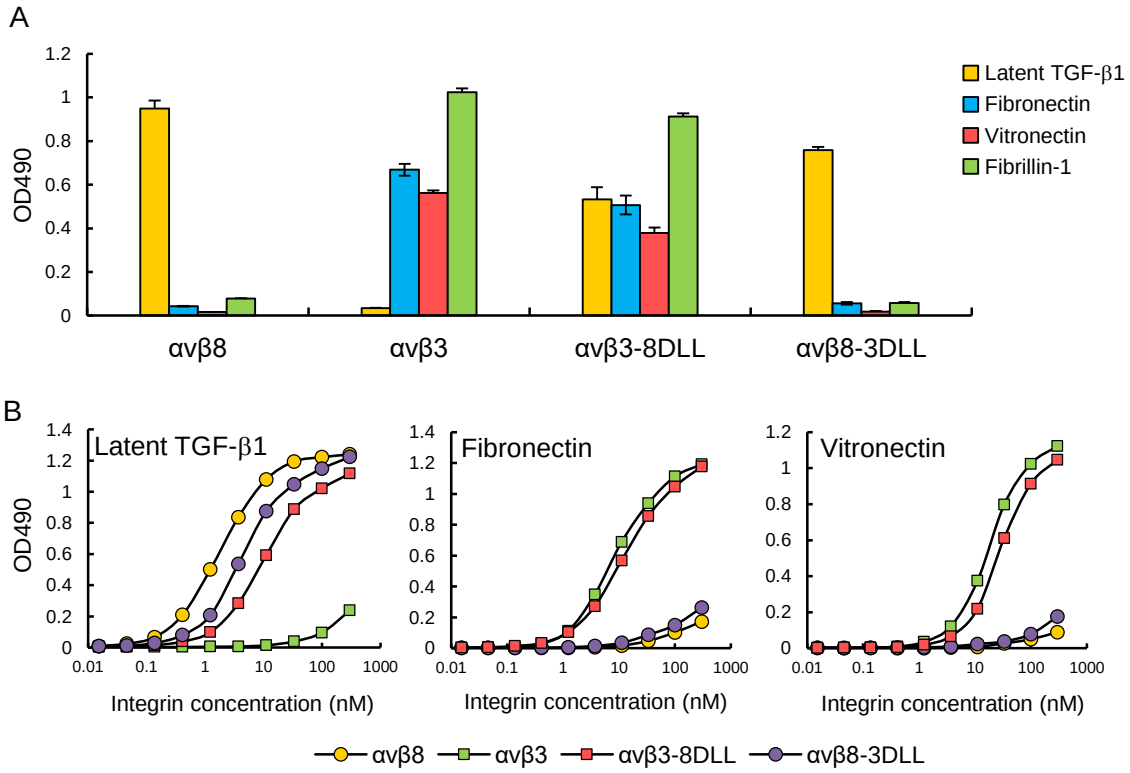

Figure 20. Ligand-binding specificities of DLL swap mutants. (*A*) Binding activities of DLL swap mutants of αvβ8 and αvβ3 integrins towards latent TGF-β1, fibronectin, vitronectin, and fibrillin-1. The results represent the means of three independent determinations. (*B*) Titration curves of DLL swap mutants bound to latent TGF-β1 (*left*), fibronectin (*middle*), and vitronectin (*right*). Increasing concentrations of αvβ8 integrin (*yellow circles*), αvβ3 integrin (*green squares*), αvβ3-8DLL (*red squares*), and αvβ8-3DLL (*purple circles*) were allowed to bind to microtiter plates coated with latent TGF- β1, fibronectin, or vitronectin in the presence of 1 mM $MnCl_2$. Bound integrins were quantified as described in the *Experimental Procedures*. Apparent dissociation constants of recombinant integrins are summarized in Table 9.

Table 9. Dissociation constants of αvβ8 integrin and its swap mutants towards latent TGF-β1

β-chains	Kd (nM)*
β8	2.3 ± 0.2
β3	ND**
β3-8DLL	ND**
β8-3DLL	4.7 ± 1.2

*Values represent the mean ± S.D. of three independent experiments.

**ND, not determined. The dissociation constant was not determined because of the partial saturation only being evaluated at the highest integrin concentration.

αvβ8 integrin, confers latent TGF-β1 binding activity to αvβ3 integrin without compromising its ability to bind to fibronectin, vitronectin, and fibrillin-1.

VIII. β8-DLL Is Not Involved in the Specific Recognition of Leu-218 Immediately after the RGD Motif—To address the apparent discrepancy of the role of β8-DLL in defining the ligand specificity of αvβ8 integrin, I examined whether β8-DLL is involved in the recognition of Leu-218 required for high-affinity binding of latent TGF-β1 to αvβ8 integrin. I examined the inhibitory effects of the RGDL and RGDA peptides on the binding of latent TGF-β1 to αvβ8-3DLL and αvβ3-8DLL, both of which were capable of binding to latent TGF-β1 (**Figure 21**). The binding of αvβ8-3DLL to latent TGF-β1 was strongly inhibited by the RGDL peptide with an IC_{50} of 0.06 μM, while substitution of the Leu residue with Ala resulted in a ~80-fold decrease in the inhibitory potency of the peptide (**Figure 21A and Table 10**). This indicated that Leu-218 is recognized by αvβ8-3DLL to sustain its specific binding to latent TGF-β1. In contrast, RGDL and RGDA peptides equally inhibited the binding of αvβ3-8DLL to latent TGF-β1 with an IC_{50} of 0.17 μM and 0.13 μM, respectively, irrespective of the presence or absence of a Leu residue immediately after the RGD motif (**Fig. 21B and Table 10**). These results demonstrated that β8-DLL in αvβ3-8DLL does not recognize the Leu residue immediately after the RGD motif, consistent with the conclusion that β8-DLL is not involved in the Leu-218-dependent high-affinity binding of αvβ8 integrin to latent TGF-β1. The RGEL peptide did not inhibit the interaction of αvβ8-3DLL and αvβ3-8DLL mutants with latent TGF-β1, highlighting the critical importance of the RGD motif in latent TGF-β1 recognition by αvβ8 integrin. Taken together, these results indicate that β8-DLL is dispensable for the specific binding of the αvβ8 integrin to latent TGF-β1, although the β8 I-like domain is necessary and sufficient for recognition of the Leu-218 residue by αvβ8 integrin.

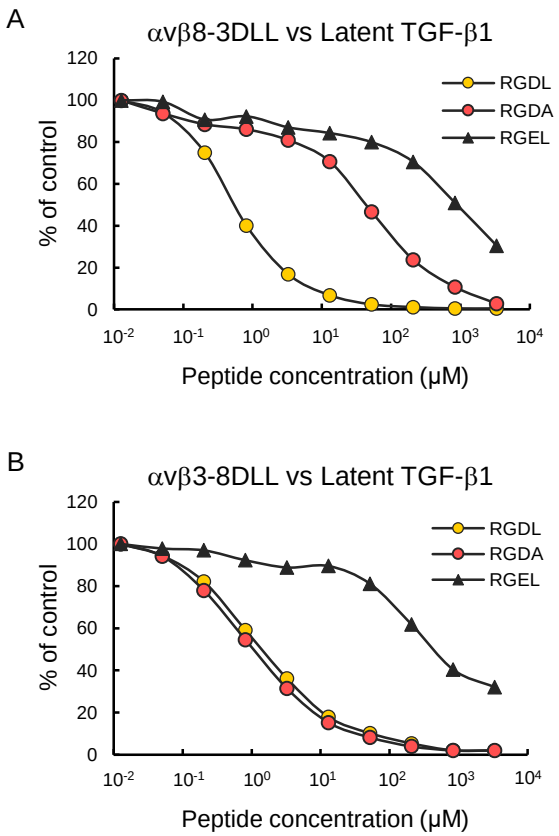

Figure 21. Inhibition of DLL swap mutant binding to latent TGF-β1 by synthetic peptides. αvβ8-3DLL (*A*) and αvβ3-8DLL (*B*) mutants (10 nM) were incubated on microtiter plates coated with latent TGF-β1 (10 nM) in the presence of increasing concentrations of synthetic peptides. To prevent precipitation of the peptides, the integrin binding assays were performed in the presence of 10% DMSO. The amounts of bound integrins are shown as percentages relative to the control, in which integrins were incubated on latent TGF-β1-coated plates in the presence of 10% DMSO. The results represent the means of three independent determinations. *Yellow circles*, RGDL (9-mer containing both RGD motif and Leu residue); *red circles*, RGDA (9-mer with the Leu→Ala substitution); *black triangles*, RGEL (9-mer with RGD → RGE substitution).

Table 10. Inhibition of ligand binding of DLL-swap mutants between αvβ3 and αvβ8 integrins by synthetic peptides

integrin vs ligand	Peptides	IC50 (μM)*
αvβ8-3DLL vs latent TGF-β1	RGDL	0.06 ± 0.02
	RGDA	4.7 ± 0.4
	RGEL	120 ± 50
αvβ3-8DLL vs latent TGF-β1	RGDL	0.17 ± 0.03
	RGDA	0.13 ± 0.03
	RGEL	46 ± 7

*Determined based on data from Figure 14. The values represent the mean ± S.D. of three independent determinations.

Discussion

This study demonstrated that αvβ8 integrin binds strongly and preferentially to latent TGF-β1 with an affinity ~100-fold higher than for other RGD proteins including fibronectin, vitronectin, and fibrillin-1. The high-affinity interaction of αvβ8 integrin with latent TGF-β1 is determined by the Leu-218 residue immediately following the RGD motif within the LAP of latent TGF-β1. Substitution of the Leu-218 residue with Ala resulted in a dramatic reduction of the latent TGF-β1 binding affinity of αvβ8 integrin, even though the RGD motif remained unperturbed. Accumulating evidence indicates that the binding affinities of RGD-containing ligands towards integrins are potentiated by sequences residing outside the RGD motif. The occurrence of such an auxiliary binding sequence was originally proposed in the central cell-binding domain of fibronectin, where a set of residues within the 9th type III repeat (designated 'synergy site') potentiates the α5β1 integrin-mediated cell-adhesive activity of the RGD motif within the 10th type III repeat (Aota et al., 1994), although electron microscopic analyses failed to confirm a direct interaction of the 9th type III module harboring the synergy site with α5β1 integrin (Takagi et al., 2003). Nephronectin also contains an auxiliary sequence LFEIFEIER required for the high-affinity binding of nephronectin to α8β1 integrin, which functions in concert with an RGD motif (Sato et al., 2009). DiCara et al. (2007) reported that the interaction of latent TGF-β1 with αvβ6 integrin is determined by an LXXI sequence immediately C-terminal to the RGD motif, in which two hydrophobic residues Leu-218 and Ile-221 form an α-helical structure and are required for the high-affinity binding of latent TGF-β1 to αvβ6 integrin. Our results show that Leu-218 is critically required for latent TGF-β1 recognition by αvβ8 integrin, but Ile-221 is dispensable for recognition, because the substitution of Ile-221 with Ala did not affect the high-affinity binding of latent TGF-β1 to αvβ8 integrin. In support of this conclusion, a 9-mer peptide containing an RGDL sequence

strongly inhibited the interaction of latent TGF-β1 with αvβ8 integrin while a 9-mer peptide with an RGDA sequence had a ~60-fold lower inhibitory effect on the interaction. The critical role of Leu-218 in latent TGF-β1 recognition by αvβ8 integrin was further corroborated by site-directed mutagenesis of fibronectin, in which the high-affinity binding toward αvβ8 integrin was conferred on fibronectin by substitution of its RGDS motif with an RGDL sequence. The Leu-218 residue immediately following the RGD motif is conserved in latent TGF-β1 among mammals, underscoring the importance of Leu-218 as an auxiliary recognition residue defining the high-affinity interaction of latent TGF-β1 with αvβ8 integrin.

I. Possible Mechanisms for the Recognition of the Lue-218 Residue by the Integrin β8 I-like Domain

The high-affinity binding of αvβ8 integrin with latent TGF-β1 was conferred upon αvβ3 integrin (which normally exhibits marginal latent TGF-β1 binding) by swapping the I-like domain of the β3 subunit with that of the β8 subunit. This demonstrated the β I-like domain primarily defines the high-affinity interaction of αvβ8 integrin with latent TGF-β1. Dong et al. (2014) reported the crystal structure of αvβ6 integrin complexed with an 11-mer peptide HGRGDLGRLKK derived from a latent TGF-β3 peptide. They demonstrated that the β6 I-like domain interacted with the LGRLK sequence immediately following the RGD motif, which forms an amphipathic α-helix and confers high-affinity binding of αvβ6 integrin to latent TGF-β3. The binding to latent TGF-β1 by αvβ3-8BI, in which the I-like domain of β3 subunit was swapped with the β8 subunit, was strongly inhibited by the RGDL peptide but less so by the RGDA peptide, indicating the β I-like domain of the β8 subunit might harbor the region(s) responsible for Leu-218 recognition. To explore this possibility further, I predicted the structures of the β I-like domain of αvβ8 and αvβ3 integrins complexed with an RGDL-containing peptide using SWISS-MODEL with the crystal structure of αvβ6 integrin

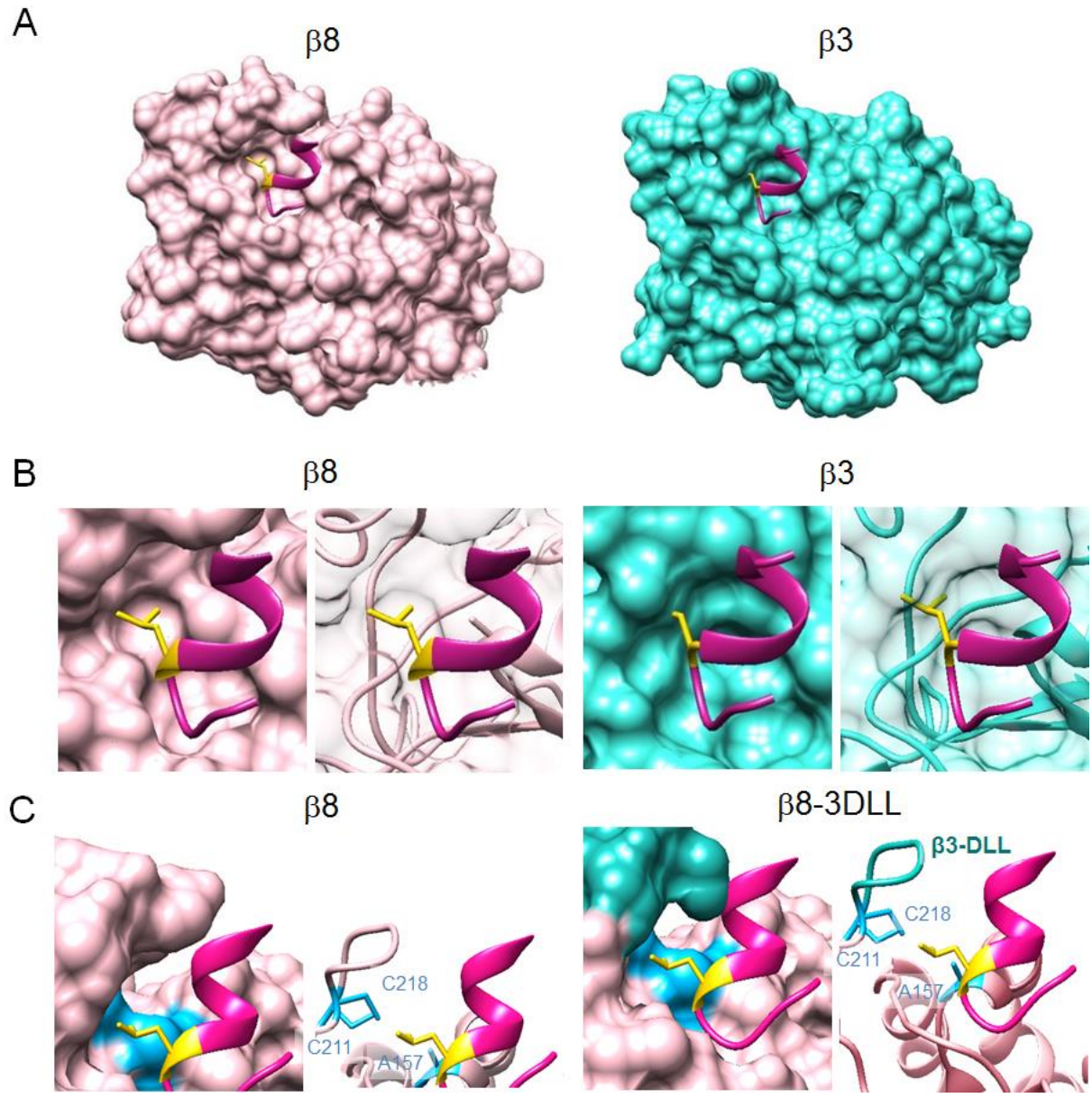

Figure 22. Predicted structures of the head region of αvβ8 integrin with an 11-mer peptide containing RGD motif and Leu residue. (*A*) Surface representation of β I-like domain of αvβ8 integrin (*left*) and αvβ3 integrin (*right*) with the RGDL-containing 11-mer peptide derived from latent TGF-β3 were created using the crystal structure of αvβ6 integrin with this peptide (PDB ID; 4UM9) as the template. The models were predicted with the SWISS-MODEL (http://swissmodel.expasy.org/) and fine-tuned by energy minimization with UCSF Chimera (http://www.cgl.ucsf.edu/chimera/). β I-like domains of β8 and β3 are shown in *pink* and *cyan*, respectively. 11-mer peptides are colored in *magenta*, and the Leu residue immediately following the RGD motif is shown with sidechain in *yellow*. (*B*) Close-up views of the predicted structures of β I-like domain of αvβ8 integrin (*left*) and αvβ3 integrin (*right*) with the 11-mer peptide. The β8 I-like domain is predicted to assume a structure of open conformation that allows the side chain of the Leu residue to fit into the β8 I-like domain, while the β3 I-like domain is predicted to assume a closed structure, failing to accommodate the side chain of the Leu residue. (*C*) Close-up views of the predicted interfaces between the 11-mer peptide and β I-like domains of β8 (*left*) and β8-3DLL (*right*) subunits, focusing on the side chain of the Leu residue following the RGD motif. Hydrophobic residues located around the Leu residue, *i.e.*, Ala-157, Cys-211, and Cys-218, are shown in *blue*. The β3-DLL is shown in *cyan*.

complexed with the latent TGF-β3 peptide (Dong et al., 2014) and that of αvβ3 integrin (Dong et al., 2012) as templates (**Figure 22A and B**). The β8 I-like domain was predicted to assume a structure of open conformation that allows the sidechain of the Leu residue to fit into the β8 I-like domain, thus enabling the high-affinity binding of latent TGF-β1 with αvβ8 integrin. In contrast, the β3 I-like domain was predicted to assume a closed structure, failing to accommodate the chain of the Leu residue, and therefore resulting in a low affinity binding to latent TGF-β1. The predicted structure of αvβ8 integrin complexed with the 11-mer peptide also indicates that the side of chain of the Leu residue is surrounded by hydrophobic residues, *i.e.*, Ala-157, Cys-211, and Cys-218 of the β8 subunit, suggesting that the high-affinity binding of latent TGF-β1 to αvβ8 integrin is achieved by hydrophobic interaction of Leu-218 with the β8 subunit (**Figure 22C**). Consistent with this prediction, Dong et al. (2014) demonstrated that the Leu residue immediately following RGD motif of latent TGF-β3 interacts with hydrophobic residues of β6 I-like domain, thereby conferring high-affinity binding to αvβ6 integrin.

The DLL of β I-like domain has been shown to modulate the ligand specificity of αv-containing integrins (Takagi et al., 1997b). Although cells expressing αvβ1 integrin did not bind to the substrate coated with von Willebrand factor and fibrinogen, which are high-affinity ligands for αvβ3 integrin, cells expressing the mutant αvβ1 integrin, in which β1-DLL was swapped with β3-DLL, bound to these ligands, demonstrating that the ligand-binding specificity of αvβ3 integrin can be conferred upon αvβ1 integrin by swapping the DLL. In contrast to this report, our results showed that β3-DLL had little involvement in the recognition of fibronectin, vitronectin, and fibrillin-1 by αvβ3 integrin, because ligand-binding specificities of αvβ3 integrin towards these proteins remained unchanged after DLL swapping. Furthermore, the ability of αvβ8 integrin to bind to latent TGF-β1 was retained after swapping β8-DLL with β3-DLL, indicating that β8-DLL is not the primary determinant of the specific binding of αvβ8 integrin to latent TGF-β1. Because Leu-218 is still recognized by αvβ8-3DLL,

which retains specific binding to latent TGF-β1, it seems likely that the Leu-218-binding pocket is maintained in the β8 I-like domain even after replacement of β8-DLL with β3-DLL. Consistent with this possibility, the predicted structure of αvβ8-3DLL integrin complexed with the 11-mer peptide containing RGDL sequence shows that the hydrophobic pocket comprising Ala-157, Cys-211, and Cys-218 remains undisturbed after DLL swapping (**Figure 22C**). However, why β8-DLL confers latent TGF-β1-binding activity to αvβ3 integrin, despite β8-DLL being dispensable for the recognition of latent TGF-β1 by αvβ8 integrin, remains to be elucidated. The replacement of β3-DLL with β8-DLL might alter the conformation of the β3 I-like domain so that the resulting β I-like domain adopts a structure reminiscent to the open conformation that is competent for latent TGF-β1 binding, whereas the normal β3 I-like domain assumes a closely packed structure that constrains accommodation of Leu-218.

II. Importance of the β Hybrid Domain in the Affinity Regulation of Ligand Binding

Several lines of evidence indicate that the β hybrid domain acts as a mechanical device that regulates the affinity state of integrins by rearrangement at the interface between the β I-like domain and the β-propeller domain of the α subunit, which together form the ligand binding site of integrins. Thus, binding of α5β1 integrin to its ligand causes a dramatic change in the position of the β hybrid domain relative to the β I-like domain to induce an open conformation of the integrin headpiece (Takagi et al., 2003). Xiao et al. (2004) demonstrated that the hybrid domain of the β3 subunit extends laterally away from the ligand binding site to stabilize the open headpiece conformation. Consistent with the role of the β hybrid domain in the affinity state modulation of integrins, the limiting swing-out of the β3 hybrid domain prevents αIIbβ3 integrin to bind to its high-affinity ligand fibrinogen, indicating that the swing-out of the β3 hybrid domain is required for activation of the αIIbβ3 integrin (Cheng et al., 2013). Our results showed that αvβ3-8BI/HYB and αvβ8 integrin had a similar binding affinity to latent TGF-β1, while αvβ3-8BI had a lower latent TGF-β1 binding affinity. These

results are consistent with previous studies and support the consensus that the β hybrid domain regulates, in collaboration with the β I-like domain, the conformational change of the integrin headpiece from a low- to high-affinity state for ligand binding.

III. Involvement of the β Subunit in Determination of the Ligand Specificity of Integrins

It has been widely accepted that the ligand specificity of integrins is primarily determined by their α subunit (Barczyk et al., 2010a). αv-containing integrins are considered to be promiscuous because they exhibit broad binding specificity towards a wide variety of RGD proteins. For example, αvβ3 integrin has been shown to bind to a variety of ECM ligands containing the RGD motif, including EDIL3, prothrombin, fibrillin-1, fibrillin-2, fibronectin, bone sialoprotein (IBSP), lactadherin (MFGE8), nephronectin, osteopontin, TGF-β1, thrombonspondin-1, thrombospondin-2, and vitronectin (Andersen et al., 2000; Brandenberger et al., 2001; Hidai et al., 1998; Jovanovic et al., 2008; Lawler et al., 1988; Schurpf et al., 2012; Sun et al., 1992; Yokosaki et al., 2005). Our Results showed that αvβ3, αvβ5 and αvβ6 integrins have similar ligand specificities, thus strongly binding to EDIL3, fibrillin-1, fibrillin-2, fibronectin and vitronectin, but they differ in their binding activities to bone sialoprotein, lactadherin, osteopontin and TGF-β1 depending on their β subunit. No significant binding activities were observed with these αv-containing integrins toward prothrombin, thrombospondin-1 and thrombospondin-2. In contrast to αvβ3, αvβ5, and αvβ6 integrins, αvβ8 integrin has restricted ligand specificity toward 25 RGD proteins; it strongly bound to TGF-β1, but moderately or only marginally toward other RGD proteins. These results indicate that although αvβ8 and other αv-containing integrins share the same integrin αv subunit, they displayed distinct binding specificities toward a broad range of RGD proteins, demonstrating that integrin β subunits modulate the ligand binding specificity of αv integrins by enhancing or attenuating their binding affinities toward individual ligands. The binding affinities of α6-containing integrins toward a panel of laminin isoforms also differ depending on the type of

β subunit (Nishiuchi et al., 2006), confirming the auxiliary role of the integrin β subunits in defining the ligand specificity.

IV. Distinctive Contribution of the Leu-218 Residue in Integrin Binding between αvβ6 and αvβ8 Integrins

Previous studies indicated that TGF-β1 is one of the physiological ligands for αv-containing integrins, of which αvβ6 and αvβ8 integrins have been shown to be required for the activation of TGF-β1. In this study, comprehensive binding assays of αvβ6 and αvβ8 integrins to 25 RGD proteins demonstrated that both integrins strongly bound to latent TGF-β1. However, their binding activities toward other RGD proteins were markedly different, indicating that αvβ6 and αvβ8 integrins may recognize their ligands with distinct mechanisms. The mechanisms by which αvβ6 integrin interacts with TGF-β1 have been investigated; NMR analysis revealed that the LXXL/I sequence immediately C-terminal to the RGD motif in TGF-β1 is required for the high affinity binding to αvβ6 integrin (DiCara et al., 2007). The crystal structure of the αvβ6 integrin-TGF-β3 peptide complex suggests that two hydrophobic residues within the LGRLK sequence immediately following the RGD motif form an amphipathic α-helix and interact with the β6 I-like domain (Dong et al., 2014). Consistent with these findings, our results showed that Leu-218 plays a critical role in the latent TGF-β1 recognition by αvβ8 integrin. However, neither Ile-221 residue nor α-helical structure formed by the LXXI sequence is necessary for the latent TGF-β1 recognition by αvβ8 integrin, because the substitution of Ile-221 with Pro did not compromise the ability of latent TGF-β1 to bind to αvβ8 integrin. In contrast, the Pro-substitution mutant of Ala-219 showed a significant decrease in the ability to bind to αvβ8 integrin, suggesting the possibilities that the Ala-219 directly interacts with the β8 I-like domain or presents the Leu residue in a favorable conformation to ensure the high-affinity binding of latent TGF-β1 to αvβ8 integrin. There is preliminary data showing that the substitution of Leu-218 of latent TGF-β1 with Ala (L218A)

causes a partial decrease in the binding affinity to αvβ6 integrin, compared with wild-type latent TGF-β1 (**Figure 23**). The results suggest that Leu-218 is also involved in high-affinity binding of latent TGF-β1 to αvβ6 integrin, but its contribution to high-affinity binding is less pronounced with αvβ6 integrin, compared with αvβ8 integrin.

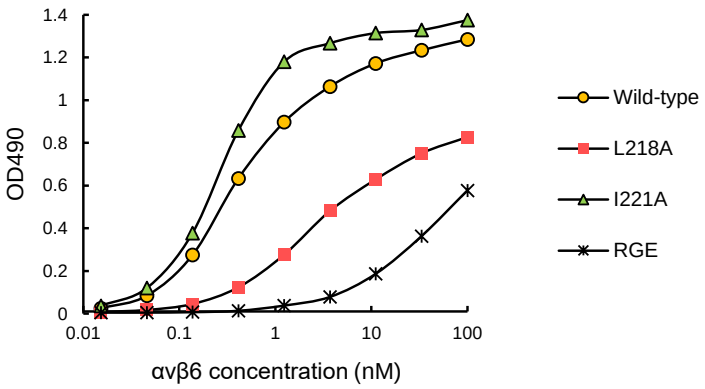

Figure 23. Effect of alanine substitutions within the LATI sequence on αvβ6 integrin-binding to latent TGF-β1. Titration curves of αvβ6 integrin bound to full-length TGF-β1 (*orange circles*), L218A substitution mutant (*red squares*), I221A substitution mutant (*green triangles*), and RGD→RGE mutant (*asterisks*). The assays were performed as described in the legend for Figure 13.

V. Problems with in silico Screening

Because αv-containing integrins bind to a variety of extracellular proteins through their RGD motifs and are highly conserved among vertebrates, putative ligands for αvβ8 integrin were extracted *in silico* from the protein sequences compiled in UniProtKB database, based on the following three criteria: 1) possession of at least one RGD sequence, 2) secretion to the extracellular space, and 3) conservation of RGD motifs among vertebrates. The resulting candidate proteins included vitronectin, an original ligand for αv integrins, fibronectin, fibrillin-1, EDIL3, lactadherin, nephronectin, osteopontin, TGF-β1, thrombospondin-1 and thrombospondin-2, and 19 other RGD-containing proteins. It should be noted, however, that some known RGD-containing integrin ligands, *e.g.*, TGF-β3, tenascin, von Willebrand factor, and fibrinogen were not included in the final list because their RGD motifs are not conserved among vertebrates. Furthermore, our *in silico* screening excluded ligands that possessed

integrin recognition sequences other than the conventional RGD motif. αIIbβ3 integrin binds to the fibrinogen γ chain through its KQAGDV sequence and α4β1 integrin binds to the fibronectin type III connecting segment-1 through its LDV sequence (Ruoslahti, 1996). I also excluded cell surface transmembrane proteins from the candidates, because most integrin ligands are secreted to the extracellular space. Therefore, I cannot rule out the possibility that unknown transmembrane proteins function as physiological ligands for αvβ8 integrin. There is evidence that transmembrane proteins such as VCAM-1, MAdCAM-1, ICAM, and E-cadherin bind to integrins and facilitate a variety of cell-cell interactions *in vivo* (Humphries et al., 2006). A screening protocol modified to include RGD-containing transmembrane proteins should provide an extended repertoire of candidates for integrin ligands, thereby increasing the chance of identifying novel ligands for αvβ8 and other αv-containing integrins.

VI. Possible Roles of Leu-218 in the Interaction of Latent TGF-β with αvβ8 Integrin

It is still unclear why αvβ8 integrin requires strictly the Leu-218 residue for selective recognition of latent TGF-β1. Here, I discuss the possible mechanisms underlying the enhancement of the affinities by Leu-218, in concert with the RGD sequence. Our study showed that Leu-218 immediately after the RGD motif is recognized by the integrin β8 I-like domain. Thus, one possibility is that Leu-218 binds to the hydrophobic residues in the β8 I-like domain, resulting in a decrease of the dissociation rate, thereby stabilizing the final complex between the integrin and latent TGFβ-1. This possibility is in agreement with the structure of αvβ6 integrin complexed with the latent TGF-β1, which was determined by X-ray crystallography (Dong et al., 2017). The structure of the complex demonstrated that the two hydrophobic residues, Leu-218 and Ile-221, bind in a hydrophobic pocket formed by the integrin β6 subunit to increase the binding affinity to αvβ6 integrin, consistent with our model that the side chain of the Leu-218 residue fits in the hydrophobic pocket of the β8 I-like domain. Another possibility is that Leu-218 regulates the conformation of the RGD motif to

stabilize the initial encounter of TGF-β1 with αvβ8 integrin. This possibility was suggested by the experiments showing that the mutation within the synergy site of fibronectin primarily affects the association rate in the binding to α5β1 integrin, but the dissociation rate is slightly affected (Takagi et al., 2003). However, the crystal structure of a dimer complex of latent TGF-β1 shows that the Leu-218 immediately following the RGD motif is not surface exposed (Shi et al., 2011), making this possibility less likely. Therefore, the former model, *i.e.*, Leu-218 stabilizes the final complex between αvβ8 integrin and latent TGF-β1 through the interaction with the hydrophobic residues in the β8 subunit, seems more reasonable than the latter model. Further studies, particularly structural analyses of the αvβ8 integrin-latent TGF-β1 complex, are required to better understand how the Leu-218 residue of latent TGF-β1 enhances the binding affinity toward αvβ8 integrin.

VIII. Roles of αvβ8 Integrin in Activation of Latent TGF-β1

There is compelling evidence that αvβ8 integrin plays a dominant role in activating latent TGF-β1 in the developing brain. Mice deficient in the expression of the integrin β8 subunit exhibit variable embryonic lethality because of vasculogenesis failure and severe brain hemorrhage (Zhu et al., 2002), as is the case with mice deficient for integrin αv subunit expression (Bader et al., 1998). Notably, when mice with a TGF-β1 gene knock-in mutation that causes an RGE substitution of the RGD motif are crossed with TGF-β3 deficient mice, they die as a result of severe brain hemorrhage (Mu et al., 2008), recapitulating the phenotype of integrin β8-deficent mice. Given the similarities in phenotypes between αvβ8 integrin-deficient mice and TGF-β1(RGE)/TGF-β3 double mutant mice, αvβ8 integrin has been proposed to act as an “angiogenic switch” in the brain through TGF-β activation (Arnold et al., 2014; Cambier et al., 2005). Consistent with the role of αvβ8 integrin in TGF-β1 activation, Yamazaki et al. (2011) reported that β8 integrin was specifically expressed by Schwann cells and involved in latent TGF-β activation in the bone marrow, thereby regulating

hematopoietic stem cell hibernation. Furthermore, the activation of latent TGF-β1 by αvβ8 integrin may occur via mechanisms distinct from those for TGF-β1 activation by αvβ6 integrin, which requires the β6 subunit cytoplasmic domain and a functional actin cytoskeleton. However, TGF-β activation by αvβ8 integrin is considered independent of the β8 subunit cytoplasmic domain and actin cytoskeleton (Mu et al., 2002; Munger et al., 1999). Indeed, the amino acid sequence of the cytoplasmic domain of integrin β8 subunit differs significantly from those of other β subunits (Moyle et al., 1991), making it unlikely that the β8 cytoplasmic domain interacts with the actin cytoskeleton and generates traction force for cell spreading and migration as well as the conformational activation of latent TGF-βs (Cambier et al., 2000). Given its restricted binding specificity and prominent expression in astrocytes surrounding cerebral blood vessels (Cambier et al., 2005), αvβ8 integrin may function as an anchor specialized for latent TGF-β1, thereby ensuring the localized action of active-TGF-β1 at the neurovascular unit where astrocytes crosstalk with endothelial cells to facilitate brain vascular development.

Conclusion

I have shown that the αvβ8 integrin binds strongly and preferentially to latent TGF-β1. Its high-affinity binding is primarily defined by the Leu-218 residue located immediately after the RGD motif within the LAP of latent TGF-β1. I have provided evidence that the Leu residue confers the αvβ8 integrin binding ability to fibronectin, highlighting the auxiliary role of Leu-218 in defining the ligand specificity to latent TGF-β1 by αvβ8 integrin. Given that the side chain of the Leu residue fits into the β8 I-like domain of integrin β8 subunit, but not of integrin β3 subunit, upon prediction of the structures of αvβ8 and αvβ3 integrins complexed with an RGDL peptide, I propose a model for the Leu-dependent recognition of latent-TGF-β1 by αv integrins, wherein the αvβ8 integrin recognizes the Leu residue immediately after the RGD motif through hydrophobic interactions, although it remains to be determined how the β8 I-like domain recognizes the Leu-218 residue at the atomic level. Further studies including the X-ray crystallography of the αvβ8 integrin complexed with a latent TGF-β1 are awaited to better understand how the Leu-218 residue is involved in the interaction of αvβ8 integrin with latent TGF-β1.

In summary, the comprehensive study on the binding activities of αvβ8 integrin and its mutant proteins towards a wide range of RGD proteins has elucidated molecular mechanisms involved in the specific recognition of latent TGF-β1 by αvβ8 integrin and established the foundation for understanding physiological and pathological roles of αvβ8 integrin.

References

Andersen, M.H., Graversen, H., Fedosov, S.N., Petersen, T.E., and Rasmussen, J.T. (2000). Functional analyses of two cellular binding domains of bovine lactadherin. Biochemistry *39*, 6200-6206.

Annes, J.P., Munger, J.S., and Rifkin, D.B. (2003). Making sense of latent TGFβ activation. J Cell Sci *116*, 217-224.

Annes, J.P., Rifkin, D.B., and Munger, J.S. (2002). The integrin αVβ6 binds and activates latent TGFβ3. FEBS Lett *511*, 65-68.

Aota, S., Nomizu, M., and Yamada, K.M. (1994). The short amino acid sequence Pro-His-Ser-Arg-Asn in human fibronectin enhances cell-adhesive function. J Biol Chem *269*, 24756-24761.

Apweiler, R., Bairoch, A., Wu, C.H., Barker, W.C., Boeckmann, B., Ferro, S., Gasteiger, E., Huang, H., Lopez, R., Magrane, M., *et al.* (2004). UniProt: the Universal Protein knowledgebase. Nucleic Acids Res *32*, D115-119.

Araya, J., Cambier, S., Morris, A., Finkbeiner, W., and Nishimura, S.L. (2006). Integrin-mediated transforming growth factor-β activation regulates homeostasis of the pulmonary epithelial-mesenchymal trophic unit. Am J Pathol *169*, 405-415.

Arnaout, M.A., Goodman, S.L., and Xiong, J.P. (2007). Structure and mechanics of integrin-based cell adhesion. Curr Opin Cell Biol *19*, 495-507.

Arnold, T.D., Niaudet, C., Pang, M.F., Siegenthaler, J., Gaengel, K., Jung, B., Ferrero, G.M., Mukouyama, Y.S., Fuxe, J., Akhurst, R., *et al.* (2014). Excessive vascular sprouting underlies cerebral hemorrhage in mice lacking αVβ8-TGFβ signaling in the brain. Development *141*, 4489-4499.

Bader, B.L., Rayburn, H., Crowley, D., and Hynes, R.O. (1998). Extensive vasculogenesis, angiogenesis, and organogenesis precede lethality in mice lacking all αv integrins. Cell *95*, 507-519.

Barczyk, M., Carracedo, S., and Gullberg, D. (2010a). Integrins. Cell Tissue Res *339*, 269-280.

Beglova, N., Blacklow, S.C., Takagi, J., and Springer, T.A. (2002). Cysteine-rich module structure reveals a fulcrum for integrin rearrangement upon activation. Nat Struct Biol *9*, 282-287.

Brandenberger, R., Schmidt, A., Linton, J., Wang, D., Backus, C., Denda, S., Muller, U., and Reichardt, L.F. (2001). Identification and characterization of a novel extracellular matrix protein nephronectin that is associated with integrin α8β1 in the embryonic kidney. J Cell Biol *154*, 447-458.

Cambier, S., Gline, S., Mu, D., Collins, R., Araya, J., Dolganov, G., Einheber, S., Boudreau, N., and Nishimura, S.L. (2005). Integrin αvβ8-mediated activation of transforming growth factor-β by perivascular astrocytes: an

angiogenic control switch. Am J Pathol *166*, 1883-1894.

Cambier, S., Mu, D.Z., O'Connell, D., Boylen, K., Travis, W., Liu, W.H., Broaddus, V.C., and Nishimura, S.L. (2000). A role for the integrin αvβ8 in the negative regulation of epithelial cell growth. Cancer Res *60*, 7084-7093.

Chen, C., Li, Z., Huang, H., Suzek, B.E., and Wu, C.H. (2013). A fast Peptide Match service for UniProt Knowledgebase. Bioinformatics *29*, 2808-2809.

Chen, Y., Dabovic, B., Annes, J.P., and Rifkin, D.B. (2002). Latent TGF-β binding protein-3 (LTBP-3) requires binding to TGF-β for secretion. FEBS Lett *517*, 277-280.

Cheng, M., Li, J., Negri, A., and Coller, B.S. (2013). Swing-out of the β3 hybrid domain is required for αIIbβ3 priming and normal cytoskeletal reorganization, but not adhesion to immobilized fibrinogen. PLoS One *8*, e81609.

Clements, J.M., Newham, P., Shepherd, M., Gilbert, R., Dudgeon, T.J., Needham, L.A., Edwards, R.M., Berry, L., Brass, A., and Humphries, M.J. (1994). Identification of a key integrin-binding sequence in VCAM-1 homologous to the LDV active site in fibronectin. J Cell Sci *107 (Pt 8)*, 2127-2135.

Crawford, S.E., Stellmach, V., Murphy-Ullrich, J.E., Ribeiro, S.M., Lawler, J., Hynes, R.O., Boivin, G.P., and Bouck, N. (1998). Thrombospondin-1 is a major activator of TGF-β1 in vivo. Cell *93*, 1159-1170.

DiCara, D., Rapisarda, C., Sutcliffe, J.L., Violette, S.M., Weinreb, P.H., Hart, I.R., Howard, M.J., and Marshall, J.F. (2007). Structure-function analysis of Arg-Gly-Asp helix motifs in αvβ6 integrin ligands. J Biol Chem *282*, 9657-9665.

Dong, X., Hudson, N.E., Lu, C., and Springer, T.A. (2014). Structural determinants of integrin β-subunit specificity for latent TGF-β. Nat Struct Mol Biol *21*, 1091-1096.

Dong, X., Mi, L.Z., Zhu, J., Wang, W., Hu, P., Luo, B.H., and Springer, T.A. (2012). αVβ3 integrin crystal structures and their functional implications. Biochemistry *51*, 8814-8828.

Dong, X., Zhao, B., Iacob, R.E., Zhu, J., Koksal, A.C., Lu, C., Engen, J.R., and Springer, T.A. (2017). Force interacts with macromolecular structure in activation of TGF-β. Nature *542*, 55-59.

Dubois, C.M., Laprise, M.H., Blanchette, F., Gentry, L.E., and Leduc, R. (1995). Processing of transforming growth factor β1 precursor by human furin convertase. J Biol Chem *270*, 10618-10624.

Emsley, J., Knight, C.G., Farndale, R.W., Barnes, M.J., and Liddington, R.C. (2000). Structural basis of collagen recognition by integrin α2β1. Cell *101*, 47-56.

Gray, A.M., and Mason, A.J. (1990). Requirement for activin A and transforming growth factor-β1 pro-regions in homodimer assembly. Science *247*, 1328-1330.

Heino, J., Massague, J. (1989). Transforming growth factor-β switches the pattern of integrins expressed in MG-63 human osteosarcoma cells and causes a selective loss of cell adhesion to laminin. J Biol Chem *264*, 21806-21811.

Heino, J., Ignotz, R.A., Hemler, M.E., Crouse, C., Massague, J. (1989). Regulation of cell adhesion receptors by transforming growth factor-β. Concomintant regulation of integrins that share a common β1 ssubunit. J Biol Chem *264*, 380-388.

Hidai, C., Zupancic, T., Penta, K., Mikhail, A., Kawana, M., Quertermous, E.E., Aoka, Y., Fukagawa, M., Matsui, Y., Platika, D., *et al.* (1998). Cloning and characterization of developmental endothelial locus-1: an embryonic endothelial cell protein that binds the αvβ3 integrin receptor. Genes Dev *12*, 21-33.

Hirokawa, T., Boon-Chieng, S., and Mitaku, S. (1998). SOSUI: classification and secondary structure prediction system for membrane proteins. Bioinformatics *14*, 378-379.

Huang, X.Z., Wu, J.F., Cass, D., Erle, D.J., Corry, D., Young, S.G., Farese, R.V., Jr., and Sheppard, D. (1996). Inactivation of the integrin β6 subunit gene reveals a role of epithelial integrins in regulating inflammation in the lung and skin. J Cell Biol *133*, 921-928.

Hubbard, T., Barker, D., Birney, E., Cameron, G., Chen, Y., Clark, L., Cox, T., Cuff, J., Curwen, V., Down, T., *et al.* (2002). The Ensembl genome database project. Nucleic Acids Res *30*, 38-41.

Humphries, J.D., Byron, A., and Humphries, M.J. (2006). Integrin ligands at a glance. J Cell Sci *119*, 3901-3903.

Hutchings, H., Ortega, N., and Plouet, J. (2003). Extracellular matrix-bound vascular endothelial growth factor promotes endothelial cell adhesion, migration, and survival through integrin ligation. FASEB J *17*, 1520-1522.

Huveneers, S., and Danen, E.H. (2009). Adhesion signaling - crosstalk between integrins, Src and Rho. J Cell Sci *122*, 1059-1069.

Hynes, R.O. (2002). Integrins: bidirectional, allosteric signaling machines. Cell *110*, 673-687.

Ido, H., Harada, K., Futaki, S., Hayashi, Y., Nishiuchi, R., Natsuka, Y., Li, S., Wada, Y., Combs, A.C., Ervasti, J.M., *et al.* (2004). Molecular dissection of the α-dystroglycan- and integrin-binding sites within the globular domain of human laminin-10. J Biol Chem *279*, 10946-10954.

Ido, H., Nakamura, A., Kobayashi, R., Ito, S., Li, S., Futaki, S., and Sekiguchi, K. (2007). The requirement of the glutamic acid residue at the third position from the carboxyl termini of the laminin γ chains in integrin binding by laminins. J Biol Chem *282*, 11144-11154.

Ignotz, R.A., Heino, J., Massague, J. (1989). Regulation of cell adhesion receptors by transforming growth factor-β. Regulation of vitronection receptor and LFA-1. J Biol Chem *264*, 389-392.

Ivaska, J., and Heino, J. (2010). Interplay between cell adhesion and growth factor receptors: from the plasma membrane to the endosomes. Cell Tissue Res *339*, 111-120.

Jovanovic, J., Iqbal, S., Jensen, S., Mardon, H., and Handford, P. (2008). Fibrillin-integrin interactions in health and disease. Biochem Soc Trans *36*, 257-262.

Kiyozumi, D., Osada, A., Sugimoto, N., Weber, C.N., Ono, Y., Imai, T., Okada, A., and Sekiguchi, K. (2005). Identification of a novel cell-adhesive protein spatiotemporally expressed in the basement membrane of mouse developing hair follicle. Exp Cell Res *306*, 9-23.

Komoriya, A., Green, L.J., Mervic, M., Yamada, S.S., Yamada, K.M., and Humphries, M.J. (1991). The minimal essential sequence for a major cell type-specific adhesion site (CS1) within the alternatively spliced type III connecting segment domain of fibronectin is leucine-aspartic acid-valine. J Biol Chem *266*, 15075-15079.

Laemmli, U.K. (1970). Cleavage of structural proteins during the assembly of the head of bacteriophage T4. Nature *227*, 680-685.

Lawler, J., Weinstein, R., and Hynes, R.O. (1988). Cell attachment to thrombospondin: the role of ARG-GLY-ASP, calcium, and integrin receptors. J Cell Biol *107*, 2351-2361.

Liu, J., Zeng, L., Kennedy, R.M., Gruenig, N.M., and Childs, S.J. (2012). βPix plays a dual role in cerebral vascular stability and angiogenesis, and interacts with integrin αvβ8. Dev Biol *363*, 95-105.

Lu, M., Munger, J.S., Steadele, M., Busald, C., Tellier, M., and Schnapp, L.M. (2002). Integrin α8β1 mediates adhesion to LAP-TGFβ1. J Cell Sci *115*, 4641-4648.

Ludbrook, S.B., Barry, S.T., Delves, C.J., and Horgan, C.M. (2003). The integrin αvβ3 is a receptor for the latency-associated peptides of transforming growth factors β1 and β3. Biochem J *369*, 311-318.

Manabe, R., Ohe, N., Maeda, T., Fukuda, T., and Sekiguchi, K. (1997). Modulation of cell-adhesive activity of fibronectin by the alternatively spliced EDA segment. J Cell Biol *139*, 295-307.

Martin, J.S., Dickson, M.C., Cousins, F.M., Kulkarni, A.B., Karlsson, S., and Akhurst, R.J. (1995). Analysis of homozygous TGFβ1 null mouse embryos demonstrates defects in yolk sac vasculogenesis and hematopoiesis. Ann N Y Acad Sci *752*, 300-308.

Moyle, M., Napier, M.A., and McLean, J.W. (1991). Cloning and expression of a divergent integrin subunit β8. J Biol Chem *266*, 19650-19658.

Mu, D., Cambier, S., Fjellbirkeland, L., Baron, J.L., Munger, J.S., Kawakatsu, H., Sheppard, D., Broaddus, V.C., and Nishimura, S.L. (2002). The integrin αvβ8 mediates epithelial homeostasis through MT1-MMP-dependent activation of TGF-β1. J Cell Biol *157*, 493-507.

Mu, Z., Yang, Z., Yu, D., Zhao, Z., and Munger, J.S. (2008). TGFβ1 and TGFβ3 are partially redundant effectors in

brain vascular morphogenesis. Mech Dev *125*, 508-516.

Munger, J.S., Harpel, J.G., Giancotti, F.G., and Rifkin, D.B. (1998). Interactions between growth factors and integrins: latent forms of transforming growth factor-β are ligands for the integrin αvβ1. Mol Biol Cell *9*, 2627-2638.

Munger, J.S., Huang, X., Kawakatsu, H., Griffiths, M.J., Dalton, S.L., Wu, J., Pittet, J.F., Kaminski, N., Garat, C., Matthay, M.A., *et al.* (1999). The integrin αvβ6 binds and activates latent TGF β1: a mechanism for regulating pulmonary inflammation and fibrosis. Cell *96*, 319-328.

Nakai, K., and Horton, P. (1999). PSORT: a program for detecting sorting signals in proteins and predicting their subcellular localization. Trends Biochem Sci *24*, 34-36.

Nermut, M.V., Green, N.M., Eason, P., Yamada, S.S., and Yamada, K.M. (1988). Electron microscopy and structural model of human fibronectin receptor. EMBO J *7*, 4093-4099.

Nishimura, S.L., Boylen, K.P., Einheber, S., Milner, T.A., Ramos, D.M., and Pytela, R. (1998). Synaptic and glial localization of the integrin αvβ8 in mouse and rat brain. Brain Res *791*, 271-282.

Nishimura, S.L., Sheppard, D., and Pytela, R. (1994). Integrin αvβ8. Interaction with vitronectin and functional divergence of the β8 cytoplasmic domain. J Biol Chem *269*, 28708-28715.

Nishiuchi, R., Takagi, J., Hayashi, M., Ido, H., Yagi, Y., Sanzen, N., Tsuji, T., Yamada, M., and Sekiguchi, K. (2006). Ligand-binding specificities of laminin-binding integrins: a comprehensive survey of laminin-integrin interactions using recombinant α3β1, α6β1, α7β1 and α6β4 integrins. Matrix Biol *25*, 189-197.

Osada, A., Kiyozumi, D., Tsutsui, K., Ono, Y., Weber, C.N., Sugimoto, N., Imai, T., Okada, A., and Sekiguchi, K. (2005). Expression of MAEG, a novel basement membrane protein, in mouse hair follicle morphogenesis. Exp Cell Res *303*, 148-159.

Pytela, R., Pierschbacher, M.D., and Ruoslahti, E. (1985a). A 125/115-kDa cell surface receptor specific for vitronectin interacts with the arginine-glycine-aspartic acid adhesion sequence derived from fibronectin. Proc Natl Acad Sci U S A *82*, 5766-5770.

Pytela, R., Pierschbacher, M.D., and Ruoslahti, E. (1985b). Identification and isolation of a 140 kd cell surface glycoprotein with properties expected of a fibronectin receptor. Cell *40*, 191-198.

Redick, S.D., Settles, D.L., Briscoe, G., and Erickson, H.P. (2000). Defining fibronectin's cell adhesion synergy site by site-directed mutagenesis. J Cell Biol *149*, 521-527.

Ricort, J.M. (2004). Insulin-like growth factor binding protein (IGFBP) signalling. Growth Horm IGF Res *14*, 277-286.

Ruoslahti, E. (1996). RGD and other recognition sequences for integrins. Annu Rev Cell Dev Biol *12*, 697-715.

Sato-Nishiuchi, R., Nakano, I., Ozawa, A., Sato, Y., Takeichi, M., Kiyozumi, D., Yamazaki, K., Yasunaga, T., Futaki, S., and Sekiguchi, K. (2012). Polydom/SVEP1 is a ligand for integrin α9β1. J Biol Chem *287*, 25615-25630.

Sato, Y., Uemura, T., Morimitsu, K., Sato-Nishiuchi, R., Manabe, R., Takagi, J., Yamada, M., and Sekiguchi, K. (2009). Molecular basis of the recognition of nephronectin by integrin α8β1. J Biol Chem *284*, 14524-14536.

Schneider, H., Harbottle, R.P., Yokosaki, Y., Kunde, J., Sheppard, D., and Coutelle, C. (1998). A novel peptide, PLAEIDGIELTY, for the targeting of α9β1-integrins. FEBS Lett *429*, 269-273.

Schurpf, T., Chen, Q., Liu, J.H., Wang, R., Springer, T.A., and Wang, J.H. (2012). The RGD finger of Del-1 is a unique structural feature critical for integrin binding. FASEB J *26*, 3412-3420.

Sekiguchi, K., and Hakomori, S. (1983). Domain structure of human plasma fibronectin. Differences and similarities between human and hamster fibronectins. J Biol Chem *258*, 3967-3973.

Sheppard, D., Cohen, D.S., Wang, A., Busk, M. (1992). Transforming growth factor β differentially regulates expression of integrin subunits in guinea pig airway epithelial cells. J Biol Chem *267*, 17409-17414.

Shi, M., Zhu, J., Wang, R., Chen, X., Mi, L., Walz, T., and Springer, T.A. (2011). Latent TGF-β structure and activation. Nature *474*, 343-349.

Soro, S., Orecchia, A., Morbidelli, L., Lacal, P.M., Morea, V., Ballmer-Hofer, K., Ruffini, F., Ziche, M., D'Atri, S., Zambruno, G., *et al.* (2008). A proangiogenic peptide derived from vascular endothelial growth factor receptor-1 acts through α5β1 integrin. Blood *111*, 3479-3488.

Streuli, C.H., and Akhtar, N. (2009). Signal co-operation between integrins and other receptor systems. Biochem J *418*, 491-506.

Sun, X., Skorstengaard, K., and Mosher, D.F. (1992). Disulfides modulate RGD-inhibitable cell adhesive activity of thrombospondin. J Cell Biol *118*, 693-701.

Takada, Y., Ye, X., and Simon, S. (2007). The integrins. Genome Biol *8*, 215.

Takagi, J. (2007). Structural basis for ligand recognition by integrins. Curr Opin Cell Biol *19*, 557-564.

Takagi, J., Erickson, H.P., and Springer, T.A. (2001). C-terminal opening mimics 'inside-out' activation of integrin α5β1. Nat Struct Biol *8*, 412-416.

Takagi, J., Kamata, T., Meredith, J., Puzon-McLaughlin, W., and Takada, Y. (1997a). Changing ligand specificities of αvβ1 and αvβ3 integrins by swapping a short diverse sequence of the β subunit. J Biol Chem *272*, 19794-19800.

Takagi, J., Kamata, T., Meredith, J., Puzon-McLaughlin, W., and Takada, Y. (1997b). Changing ligand specificities of αvβ1 and αvβ3 integrins by swapping a short diverse sequence of the β subunit. J Biol Chem *272*,

19794-19800.

Takagi, J., Strokovich, K., Springer, T.A., and Walz, T. (2003). Structure of integrin α5β1 in complex with fibronectin. EMBO J *22*, 4607-4615.

Taniguchi, Y., Li, S., Takizawa, M., Oonishi, E., Toga, J., Yagi, E., and Sekiguchi, K. (2017). Probing the acidic residue within the integrin binding site of laminin-511 that interacts with the metal ion-dependent adhesion site of α6β1 integrin. Biochem Biophys Res Commun *487*, 525-531.

Tatti, O., Vehvilainen, P., Lehti, K., and Keski-Oja, J. (2008). MT1-MMP releases latent TGF-β1 from endothelial cell extracellular matrix via proteolytic processing of LTBP-1. Exp Cell Res *314*, 2501-2514.

Van der Flier, A., and Sonnenberg, A. (2001). Function and interactions of integrins. Cell Tissue Res *305*, 285-298.

Venstrom, K., and Reichardt, L. (1995). β8 integrins mediate interactions of chick sensory neurons with laminin-1, collagen IV, and fibronectin. Mol Biol Cell *6*, 419-431.

Verdone, G., Doliana, R., Corazza, A., Colebrooke, S.A., Spessotto, P., Bot, S., Bucciotti, F., Capuano, A., Silvestri, A., Viglino, P., *et al.* (2008). The solution structure of EMILIN1 globular C1q domain reveals a disordered insertion necessary for interaction with the α4β1 integrin. J Biol Chem *283*, 18947-18956.

Vlahakis, N.E., Young, B.A., Atakilit, A., Hawkridge, A.E., Issaka, R.B., Boudreau, N., and Sheppard, D. (2007). Integrin α9β1 directly binds to vascular endothelial growth factor (VEGF)-A and contributes to VEGF-A-induced angiogenesis. J Biol Chem *282*, 15187-15196.

Walton, K.L., Makanji, Y., Chen, J., Wilce, M.C., Chan, K.L., Robertson, D.M., and Harrison, C.A. (2010). Two distinct regions of latency-associated peptide coordinate stability of the latent transforming growth factor-β1 complex. J Biol Chem *285*, 17029-17037.

Worthington, J.J., Klementowicz, J.E., and Travis, M.A. (2011). TGFβ: a sleeping giant awoken by integrins. Trends Biochem Sci *36*, 47-54.

Xiao, T., Takagi, J., Coller, B.S., Wang, J.H., and Springer, T.A. (2004). Structural basis for allostery in integrins and binding to fibrinogen-mimetic therapeutics. Nature *432*, 59-67.

Xiong, J.P., Stehle, T., Diefenbach, B., Zhang, R., Dunker, R., Scott, D.L., Joachimiak, A., Goodman, S.L., and Arnaout, M.A. (2001). Crystal structure of the extracellular segment of integrin αvβ3. Science *294*, 339-345.

Xiong, J.P., Stehle, T., Zhang, R., Joachimiak, A., Frech, M., Goodman, S.L., and Arnaout, M.A. (2002). Crystal structure of the extracellular segment of integrin αvβ3 in complex with an Arg-Gly-Asp ligand. Science *296*, 151-155.

Yamazaki, S., Ema, H., Karlsson, G., Yamaguchi, T., Miyoshi, H., Shioda, S., Taketo, M.M., Karlsson, S., Iwama, A., and Nakauchi, H. (2011). Nonmyelinating Schwann cells maintain hematopoietic stem cell hibernation in the

bone marrow niche. Cell *147*, 1146-1158.

Yang, Z., Mu, Z., Dabovic, B., Jurukovski, V., Yu, D., Sung, J., Xiong, X., and Munger, J.S. (2007). Absence of integrin-mediated TGFβ1 activation in vivo recapitulates the phenotype of TGFβ1-null mice. J Cell Biol *176*, 787-793.

Yokosaki, Y., Matsuura, N., Higashiyama, S., Murakami, I., Obara, M., Yamakido, M., Shigeto, N., Chen, J., and Sheppard, D. (1998). Identification of the ligand binding site for the integrin α9β1 in the third fibronectin type III repeat of tenascin-C. J Biol Chem *273*, 11423-11428.

Yokosaki, Y., Tanaka, K., Higashikawa, F., Yamashita, K., and Eboshida, A. (2005). Distinct structural requirements for binding of the integrins αvβ6, αvβ3, αvβ5, α5β1 and α9β1 to osteopontin. Matrix Biol *24*, 418-427.

Zambruno, G., Marchisio, P.C., Marconi, A., Vaschieri, C., Melchiori, A., Giannetti, A., DeLuca, M. (1995). Transforming growth factor-β1 modulates β1 and β5 integrin receptor and induces the de novo expression of the αvβ6 heterodimer in normal human keratinocytes: implication for wound healing. J Cell Biol *129*, 853-865.

Zhu, J., Motejlek, K., Wang, D., Zang, K., Schmidt, A., and Reichardt, L.F. (2002). β8 integrins are required for vascular morphogenesis in mouse embryos. Development *129*, 2891-2903.

List of Publications

[Original Articles]

1. Miyoshi K, Mori H, Mizobe Y, Akasaka E, Ozawa A, Yoshida M, Sato M. (2009). Development of a Noninvasive Monitoring System for Evaluation of *Oct-3/4* Promoter Status in Miniature Pig Somatic Cell Nuclear Transfer Embryos. J. Reprod. Dev. *55*:661-669.
2. Ozawa, A., Akasaka, E., Watanabe, S., Yoshida, M., Miyoshi, K., and Sato, M. (2010). Usefulness of a non-invasive reporter system for monitoring reprogramming state in pig cells: results of a cell fusion experiment. J. Reprod. Dev. *56*:363-369.
3. Akasaka E, Ozawa A, Mori H, Mizobe Y, Yoshida M, Miyoshi K, Sato M. (2011). Whole-genome amplification-based GenomiPhi for multiple genomic analysis of individual early porcine embryos. Theriogenology. *75*:1543-1549.
4. Miyoshi K, Mori H, Mizobe Y, Akasaka E, Ozawa A, Yoshida M, Sato M. (2012). Valproic Acid Improves the *In Vitro* Development Competence of Bovine Somatic Cell Nuclear Transfer Embryos. Cell Reprogram. *14*:138–145.
5. Sato-Nishiuchi, R., Nakano, I., Ozawa, A., Sato, Y., Taniguchi, M., Kiyozumi, D., Yamazaki, K., Yasunaga, T., Futaki, S., and Sekiguchi, K. (2012). Polydom/SVEP1 is a ligand for integrin α9β1. J. Biol. Chem. *287*:25615-25630.
6. **Ozawa, A., Sato, Y., Imabayashi, T., Uemura, T., Takagi, J., and Sekiguchi, K. (2016). Molecular basis of the ligand binding specificity of αvβ8 integrin. J. Biol. Chem. *291*:11551-11565.**

Acknowledgement

It is a genuine pleasure to express my deep sense of thanks and gratitude to my mentor, philosopher and guide Prof. Kiyotoshi Sekiguchi of the Laboratory for Extracellular Matrix Biochemistry (now Division of Matrixome Research and Application), Institute for Protein Research, Osaka University. His firm guidance, essential criticism, and kind consideration have helped me to a very great extent to accomplish my thesis.

I would like to express my sincere gratitude to Dr. Junichi Takagi for his great suggestions and comments in my work and dissertation. I owe a deep sense of gratitude to Dr. Sato Yuya, a postdoctoral research fellow, National Institute for Health, United States of America. His timely advice with kindness, meticulous scrutiny, scholarly advice and scientific approach have enabled me to complete this task. I thank profusely Dr. Masashi Yamada, Dr. Sugiko Futaki, Mr. Tsukasa Imabayashi, Mr. Toshihiko Uemura, and all members in the Laboratory for Extracellular Matrix Biochemistry for their kind help and co-operation throughout my study period. I am extremely thankful to Dr. Masato Okada, and Dr. Hiroaki Miki for their review of my dissertation.

To all of my friends and family who provided support and encouragement.

Akio Ozawa

Institute for Protein Research, Osaka University, July 2018